Spin-Transfer Switching in Magnetic Multilayers

By

Inti Antonio Nicolás Sodemann Villadiego

Físico
Universidad Nacional de Colombia 2007

Submitted in Partial Fulfillment of the Requirements

for the Degree of Master of Sciences in

Physics

College of Arts and Sciences

University of South Carolina

2009

Accepted by:

Yaroslaw Bazaliy, Major Professor

James Knight, Second Reader

James Buggy, Interim Dean of the Graduate School

Dedication

A mi Familia

Acknowledgments

There are many people I feel indebted to and I would like to acknowledge their support during this time at University of South Carolina.

For my advisor Professor Yaroslaw Bazaliy words will be insufficient to express my immense gratitude. During this time I have undergone a process of scientific and personal growth, learning from him not only a myriad of things about the physical phenomena we are studying, but most importantly many invaluable lessons on how to do research in physics. He is not only a terrific physicist but a great human being and I have deeply enjoyed being under his advisement during this time.

Professors Alonso Botero, James Knight, Richard Creswick, Pawel Mazur and Kuniharu Kubodera, have been not only teachers but inspirational figures, which, with their knowledge and skills, have reminded me that the true learning relation is not rooted in the formalities of classes and exams but on natural forces embedded in human nature that keep us always thirsty for knowledge and understanding. I am happy to have learned from all of them.

I would like to thank as well all the members of the Condensed Matter Group working in magnetism in the nanoscale, in particular Dr. Samir Garzon whose scientific attitudes have gained my admiration and was always willing to help me solving problems that I encountered in my research.

For Ari I have no words to express what I feel. Her seemingly limitless amounts of patience with my addiction to physics are beyond my comprehension. Her company in these times has been an invaluable asset in this endeavor.

I am greatly thankful to all my friends, Alejandro, Andres, Asami, Blanca, Bochen, Camila, Julian, Mike, Mauro, Norma, Samir, Sandra, Vladimir, Yunjing, ..., who have given me their support and comprehension, and have made this time in Columbia so enjoyable.

Abstract

We study the spin transfer torque in nanoscale devices containing layers of ferromagnetic materials separated by normal metals. This phenomenon, which arises from the transfer of spin angular momentum of the conduction electrons to the localized electrons in the ferromagnet, can be used to switch the magnetization direction between different equilibrium orientations corresponding to local minima of magnetic energy.

We derive a function representing the ability of spin torque to induce switching, which turns out to be the divergence of the spin transfer torque. This result is applied to study switching in a bistable metallic nanopillar device.

We also address the question of the stabilization of magnetization directions which correspond to saddle points of the magnetic energy and find that in the generic case such stabilization is not possible and the saddles simply merge with stable equilibria as the current is increased. Nevertheless, under special conditions saddles can be stabilized by increasing the current either in a process in which they exchange their stability nature with distant equilibria or in a collision-like process with an approaching stable equilibrium. These processes are illustrated in the spin flip transistor.

Contents

List of Figures

Introduction

Spintronics, a neologism for spin transport electronics, is a term used to describe an emerging field in physics and engineering which exploits the interplay between spin dependent transport of electrons in materials and their magnetic properties. Several studies of spin dependent transport properties had been done before the 80's but the main catalyst that fueled an increased involvement in these topics was the discovery of the Giant Magnetoresistance (GMR) effect by Peter Grünberg et. al. (Binasch et al., 1989) and Albert Fert et. al. (Baibich et al., 1988), and the subsequent development of the device known as spin valve by researchers at IBM, succesfuly incorporated in the read heads of hard disk drives which lead to a tremendous explosion in their storage capacity. GMR is the increment of the resistivity of a system of metallic ferromagnetic layers separated by paramagnetic metals when their magnetization is antiparallel as compared to the resistance for parallel magnetizations, and its origin is rooted in the spin dependent electron scattering in the multilayers.

In 1996 two independent theoretical studies by Luc Berger (Berger, 1996) and John Slonczewski (Slonczewski, 1996), predicted that in a structure like those for which GMR had been observed not only the flow of electrons would be affected by the relative orientation of the magnetizations of the ferromagnets, but a reciprocal reaction would accompany this effect consisting of a torque acting on the ferromagnets trying to change their magnetization directions. This phenomenon, known as spin transfer torque, would arise as a reaction to the torque that the conduction electrons experience after entering a ferromagnet with a polarization direction diferent from that of the local magnetization.

Following this prediction the first experimental observations of spin transfer torques came from resistance changes for current driven magnetic excitations in point contact devices (Tsoi et al., 1998). Subsequent experimental studies confirmed the existence of spin torque induced magnetization switching (Sun, 1999; Wegrowe et al., 1999; Myers et al., 1999). The current controlled magnetization switching openned the possibility of building a magnetic bit element, in which the spin transfer torque would be the base for the writing mechanism and the GMR the base for the reading mechanism. One of the ideas that makes this proposal compelling is that the magnetization state of these bits can be kept without any external energy source, provided they are suffciently stable to resist thermal induced switching, and therefore they could be the basis for a non-volatile magnetic RAM. An even more ingenious spin torque based memory device, called the racetrack memory, has been proposed by Stuart Parkin (Parkin, 2004; Parkin et al., 2008), which makes use of magnetic domain walls states as bits which are stored in a long magnetic stripe and the spin transfer induced motion of the walls is used to shift the bits through the reading and writing elements.

The present work is concerned with the stability of magnetic states and the spin torque induced switching in magnetic layers whose dimensions are small enough as to consider them monodomain bodies, these scales are typically $5nm$ for their thickness and $100nm$ for their lateral sizes and the theoretical framework employed to describe them is known as macrospin model. Even though a considerable amount of theoretical and experimental studies have been done for these systems and a clear picture of the basic phenomena is currently available, there are important problems and questions ahead to be solved. From the perspective of applicability to memory devices, the two main challenges can be sumarized as follows: how to reduce the critical switching current and consequently the energy dissipated during switching, and, how to reduce the switching time, these objectives should be met without harming the inherent magnetic stability of the device to thermal fluctuations. From the perspective of fundamental understading of spin transfer, several debates are still

open, this is particularly related to the fact that the experimental observation of spin torque related effects is basically confined to resistivity measurements (which can be related to the relative orientation of the magnetizations in the multilayer system via the GMR effect), this rather limited access to the state of the system makes difficult to discriminate between different proposals for the spin transfer efficiency [1].

In this thesis we intend to introduce a function that quantifies the switching ability of the spin transfer torque in the context of the macrospin model, this quantity turns out to be the divergence of the spin torque and quantifies the tendency of spin torque to stabilize/destabilize configurations which are local minima and maxima of magnetic energy. We also address a relatively less explored scenario, the stabilization of equilibria corresponding to saddle points of magnetic energy, and find that this can be accomplished for special configurations.

This work is written in a relatively self contained manner, in the first chapter, I will introduce the basic theoretical ideas and the model required to describe the system of our interest, which is a device made of two ferromagnetic layers separated by a metal spacer through which an electric current is passed, known as metallic nanopillar. In the second chapter I will introduce the idea of divergence of spin torque as a measure of its switching ability and discuss the problem of saddle point stabilization and saddle-center merging, defining the conditions for a particular merging known as transcritical bifurcation to occur. The third chapter will illustrate the general ideas introduced in the second one, in particular the nanopillar with an in-plane external magnetic field will serve as a test for the idea of switching ability of spin torque and the spin flip transistor will illustrate the saddle point stabilization and transcritical bifurcations. A final section will close summarizing the main results and conclusions of this work.

[1] In magnetic tunnel junctions (ferromagnetic multilayers separated by insulators) the situation is more complicated because of the strong intrinsic bias dependence of the conductivity, and still a complete functional form for the spin torque is missing.

Chapter 1

Magnetism in Nanometer Scale Systems

1.1. Origin of Ferromagnetism in Transition Metals

The ability of materials to display a macroscopic magnetization in the absence of externally applied magnetic fields is known as ferromagnetism [1]. Ferromagnetism has its origin in the ordering that the spin of the electrons in these materials collectivelly develop when the temperature drops below a critical value known as Curie temperature. Below this temperature, the electrons of neighboring ions tend to align their spins along a common direction, resulting in a local non-vanishing magnetization. The interaction that underlies this phenomenon is not any explicit spin-dependent coupling of the electrons, like the dipole-dipole interactions or spin-orbit coupling, but a cooperation of the usual electrostatic Coulomb repulsion between electrons and the Pauli exclusion principle, commonly referred to as exchange interaction (Ashcroft and Mermin, 1976).

This interaction is responsible as well for the presence of spontaneus magnetization in individual atoms and molecules, in particular an isolated atom with partially filled orbitals will, in general, have a nonvanishing magnetic moment in its ground state, as described by Hund's rules. Nevertheless, this magnetic moment disappears for most of the materials when the atom is placed in a metallic crystalline environment. For most metals the appearance of band structure tends to suppress the formation of magnetic moments, the main reason being the great modifications that the metallic

[1] This definition encompasses the so-called ferrimagnetic materials, which sometimes are classified as a category on its own.

phase poses to the electron repulsion, which strongly supresses the exchange interaction otherwise present in the free atoms. In spite of this, some transition metals like iron or cobalt, are able to retain a considerable amount exchange interaction in the presence of band formation and then constitute examples of metallic ferromagnets. The exchange interaction in these materials generates a self consistent shift of the bands into majority-electron-spin band and minority-electron-spin band each containing electrons aligned in a common direction with the majority bands having lower energy (Ralph and Stiles, 2008). This energy difference results in a unbalance of spin populations which gives rise to a local magnetization.

1.2. Micromagnetic Description of Magnetization Dynamics

In a macroscopic sample of ferromagnetic material the magnetization is not uniform, but rather it is divided into small regions called magnetic domains in which the magnetization is approximately uniform, the reason for these nonuniformities is mainly the dipole coupling that builds up between different regions of the ferromagnet, this coupling between any two regions favors the antiparallel alignment of their magnetic moments and therefore competes with the exchange interaction in the larger scales.

To describe these spatial non-uniformities of the magnetization in a ferromagnet, that start appearing typically at the scale of 10 - 100 nm, a phenomenological description, commonly called micromagnetics, is introduced. In this description the magnetization is represented by a continuous vector field $\mathbf{M}(\mathbf{r})$. The free energy functional associated with $\mathbf{M}(\mathbf{r})$ can be built by adding up the contributions of different sources of magnetic energy. These sources are generally four: the interaction with any external magnetic field, the magnetocrystalline anisotropy energy, the micromagnetic exchange, and the previously mentioned dipole interaction of the magnetostatic field generated by $\mathbf{M}(\mathbf{r})$ itself (Ralph and Stiles, 2008). The magnetocrystalline anisotropy energy arises from the spin-orbit coupling and tends to align the magnetization along particular lattice directions. The micromagnetic exchange is a residual interaction of the microscopic exchange electron interaction and tends to mantain the direction of the magnetization uniform in the ferromagnet. The explicit form of the energy functional containing these interactions [2]

[2]For simplicity we have assumed the magnetocrystalline anisotropy to be uniaxial.

$$E[M] = -\mu_0 \int d^3\mathbf{r}\mathbf{H}_{ext}\cdot\mathbf{M}(\mathbf{r}) - \frac{K_a}{M_s^2}\int d^3\mathbf{r}(\hat{a}\cdot\mathbf{M}(\mathbf{r}))^2 + \frac{A_{ex}}{M_s^2}\int d^3\mathbf{r}\sum_i\left(\frac{\partial}{\partial r_i}\mathbf{M}\right)^2 - \frac{\mu_0}{8\pi}\int d^3\mathbf{r}\int d^3\mathbf{r}'\mathbf{M}(\mathbf{r})\cdot\frac{3(\mathbf{M}(\mathbf{r}')\cdot\mathbf{x})\mathbf{x} - \mathbf{M}(\mathbf{r}')|\mathbf{x}|^2}{|\mathbf{x}|^5}, \tag{1}$$

where $\mathbf{x} = \mathbf{r} - \mathbf{r}'$, $r_i = x, y, z$, $\mathbf{H}_{ext}$ is the external magnetic field, M_s is the saturation magnetization, A_{ex} is the exchange constant, K_a is the anisotropy constant, $\hat{a}$ is the easy-axis anisotropic direction [3]. In micromagnetics it is commonly assumed that $\mathbf{M}(\mathbf{r})$ only changes direction with position, retaining its magnitude equal to the saturation magnetization M_s at any point. In some way the ferromagnetic phase arranges itself to penalize strongly any small deviation in magnetization magnitude with large energy increments in way analogous to that in which the liquid phase strongly penalizes any density change. The equilibrium configurations of the magnetization would be those that extremize the energy functional. The functional differentiation of equation (1) leads to an integro-differential equation for which finding exact analytical solutions is in general not possible, and in fact the equilibrium magnetization distrubution may contain highly complex patterns such as vortices and domain walls.

To describe the magnetization dynamics an effective magnetic field, $\mathbf{H}_{eff}(\mathbf{r})$, is introduced (Lifshitz and Pitaevskii, 1981; Ralph and Stiles, 2008)

$$\mu_0\mathbf{H}_{eff}(\mathbf{r}) = -\frac{\delta E}{\delta\mathbf{M}(\mathbf{r})}, \tag{2}$$

which for the case of the magnetic energy of equation (1) reduces to

$$\mathbf{H}_{eff} = \mathbf{H}_{ext} + \frac{2K_a}{\mu_0 M_s^2}\hat{a}(\hat{a}\cdot\mathbf{M}(\mathbf{r})) + \frac{2A_{ex}}{\mu_0 M_s^2}\nabla^2\mathbf{M} + \frac{1}{4\pi}\int d^3\mathbf{r}\frac{3(\mathbf{M}(\mathbf{r}')\cdot\mathbf{x})\mathbf{x} - \mathbf{M}(\mathbf{r}')|\mathbf{x}|^2}{|\mathbf{x}|^5}. \tag{3}$$

[3] This energy functional and the rest of equations in this work are in SI units (except for a footnote referring to equation (28)).

This field generates a torque density on the local magnetic moments given by $\mu_0 \mathbf{M} \times \mathbf{H}_{eff}$, this torque gives the rate of change for the total angular momentum density of the electrons in the ferromagnet which is the source of the magnetization $\mathbf{M}(\mathbf{r})$. In the simplest case, and fortunately the most common for the magnetic multilayers of our interest, the angular momentum density equals the electron spin density, $\mathbf{S}$, and the rate of change of the magnetization is proportional to the torque density [4]

$$\partial_t \mathbf{M} = -\gamma_0 \mu_0 \mathbf{M} \times \mathbf{H}_{eff}, \tag{4}$$

with $\gamma_0 = g\mu_B/\hbar$ being the gyromagnetic ratio of the electron, μ_B the Bohr magneton and g the g-factor of the electron [5]. Equation (4) contains no dissipation, and describes the precession of $\mathbf{M}$ around the effective field $\mathbf{H}_{eff}$. A phenomelogical dissipative term, known as Gilbert damping, may be added with the resulting equation reading as

$$\partial_t \mathbf{M} = -\gamma_0 \mu_0 \mathbf{M} \times \mathbf{H}_{eff} + \frac{\alpha}{M_s} \mathbf{M} \times \partial_t \mathbf{M}, \tag{5}$$

where α is the Gilbert damping parameter, whose value is of the order of 10^{-3} and it is dimensionless. Equation (5) is normally referred to as Landau-Lifshitz-Gilbert equation or simply LLG equation. This equation is the central mathematical object of this work, by adding a suitable term describing the spin transfer torque we will study the stabillity properties of different equilibrium configurations for the magnetization and their dependence on the parameters describing the magnetic interactions of the system.

[4] In cases for which the orbital angular momentum plays a role this proportioanlity would be broken, see e.g. Ralph and Stiles (2008).

[5] This g factor is in general material dependent and may slightly differ from the g factor of the isolated electron.

1.3. Spin Transfer Torque

In any metal, either normal or ferromagnetic, an electron spin density, $\mathbf{S}$, with an associated spin current density, $\mathbf{Q}$, may be introduced. $\mathbf{S}$ is a vectorial quantity whereas $\mathbf{Q}$ is a tensor cointaining information about both the direction of the spin density itself and the direction of its flow. Thus Q_{ij} would represent the amount of jth component of the spin flowing along the ith direction per unit area per unit time (Stiles and Zangwill, 2002).

In a material in which the electrons have no spin dependent interactions the total spin is conserved, this can be expressed as a continuity equation for $\mathbf{S}$

$$\partial_t \mathbf{S} + \nabla \cdot \mathbf{Q} = 0, \tag{6}$$

where ∇ refers to derivatives with respect to the spatial part (as opposed to the spin part). Nevertheless when spin dependent interactions exist, the spin is no longer conserved, and terms representing spin "sources" and "sinks" must be added to the right side of equation (6). If inelastic spin-flip processes are neglected together with the orbital contribution to the total angular momentum density then the rate of spin density non-conservation is the torque density, $\mathbf{N}$, and equation (6) reads as

$$\partial_t \mathbf{S} + \nabla \cdot \mathbf{Q} = \mathbf{N}. \tag{7}$$

For a ferromagnetic material, if again orbital angular momentum is neglected, the spin density is proportional to its local magnetization

$$\mathbf{M} = -\gamma_0 \mathbf{S}, \tag{8}$$

the torque density is the same that appears in the right side of LLG equation (5), therefore equation (7) can be written as:

$$\partial_t \mathbf{M} = -\gamma_0 \mu_0 \mathbf{M} \times \mathbf{H}_{eff} + \frac{\alpha}{M_s} \mathbf{M} \times \partial_t \mathbf{M} + \gamma_0 \nabla \cdot \mathbf{Q}. \tag{9}$$

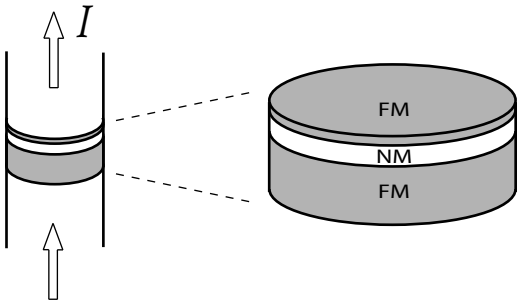

FIGURE 1.1. Typical magnetic nanopillar device with ferromagnetic (FM) and normal metal (NM) layers

When compared with equation (5) above equation suggests that the term $-\nabla \cdot \mathbf{Q}$ might be interpreted as an effective torque acting on $\mathbf{M}$ originated from the spin current flowing through the ferromagnet. We will refer to this term as a torque in the rest of this work, although we must keep in mind that this is not an actual torque acting on the spin of electrons itself in the sense defined by equation (7).
The contribution to the rate of change of $\mathbf{M}$ from $\nabla \cdot \mathbf{Q}$ contains the so-called spin transfer torque (Slonczewski, 1996; Berger, 1996; Stiles and Zangwill, 2002) and other spin dependent transport contributions like spin pumping (Tserkovnyak et al., 2002).

To be able to compute the magnetization dynamics from equation (9) it is necessary to explicitly relate $\mathbf{Q}$ and $\mathbf{M}$, this requires a theory of spin depenpent electron transport in the bulk normal and ferromagnetic metals and their interfaces. The properties of spin transport are structure and material dependent and therefore these theories need some degree of specialization into particular classes of magnetic structures and the materials from which they are made. The structures in which we will focus throughout this work are the metal-ferromagnet multilayers, in particular a device consisting of a sandwich of ferromagnet-normal metal-ferromagnet known as metallic nanopillar or spin-valve (see Figure 1.1).

Several theoretical approaches, with similar results, have been employed to compute the spin transfer torque from the spin current in metallic nanopillars [6]. Even

[6]See for example Slonczewski (1996); Bazaliy et al. (1998); Stiles and Zangwill (2002); Xiao et al. (2004); Brataas et al. (2006); Haney et al. (2008).

though the details underlying the mechanism are subtle, the basic picture is relatively simple. Conduction electrons near the Fermi surface are highly movable in the multilayer. This can be seen as follows: Fermi velocity of conduction electrons is of the order $v_F \sim 10^6 m/s$, typical thickness of magnetic layers is $d \sim 10nm$, therefore the time an electron takes to go through the layer is of the order $t_e \sim 10^{-14}s$, on the other hand the typical magnetization motion time scale is of the order $t_M \sim 1ns$ [7], thus $t_M \gg t_e$. This simple observation leads to the important approximation that for practical purposes the magnatization dynamics can be considered as "frozen" in order to compute the electron transport properties through the nanopillar.

Another relevant observation is that in order to compute the total spin transfer torque acting on the ferromagnetic layer, $\mathbf{T}_{st}$ only the values of the spin current at the interfaces are required, this is readily concluded from Gauss theorem

$$\mathbf{T}_{st} = \gamma_0 \int d^3\mathbf{r} \nabla \cdot \mathbf{Q} = \gamma_0 \int da\hat{n} \cdot \mathbf{Q}. \tag{10}$$

We consider now a simplified version of the toy model for scattering processes that occur at the normal metal-ferromagnet interface presented by Ralph and Stiles (2008). Consider a single electron incident from the normal metal into the ferromagnet with velocity normal to the interface, in such case we need to consider only three components of the spin current, Q_{xx}, Q_{yx}, Q_{zx}, and in this case $\mathbf{Q}$ can be treated as a vector. Suppose the magnetic moment of the electron points in a direction given by $\hat{s}$ (its spin therefore points along $-\hat{s}$), in this case the incident spin current density can be written as

$$\mathbf{Q}_{inc} \propto -\frac{v}{V}\frac{\hbar}{2}\hat{s}, \tag{11}$$

where v is the velocity of the electron, and V is the volume of the ferromagnetic layer. When the electron enters the ferromagnet it experiences the strong exchange

[7] This can be estimated with the frequency parameters that will appear in equation (28).

interaction generated by the electrons inside it that tend to align its magnetic moment with the local magnetization direction $\hat{m}$, therefore the electron rapidly aligns its magnetic moment with the magnetization [8], so that after a few lattice spacings the transmitted spin current is

$$\mathbf{Q}_{trans} \propto -\frac{v}{V}\frac{\hbar}{2}\hat{m}. \tag{12}$$

From equation (10) we can obtain the total spin transfer torque acting on the ferromagnet as

$$\mathbf{T}_{st} = \gamma_0 A(\mathbf{Q}_{trans} - \mathbf{Q}_{inc}) \propto \gamma_0 \frac{\hbar A v}{2V}(\hat{s} - \hat{m}), \tag{13}$$

where A is the transverse area of the nanopillar. Using Lagrange's formula we can write $\hat{s} = \hat{m}(\hat{m} \cdot \hat{s}) + \hat{m} \times (\hat{s} \times \hat{m})$, therefore omitting the component of $\mathbf{T}_{st}$ parallel to $\hat{m}$ [9], we obtain the following expression for the spin transfer torque

$$\mathbf{T}_{st} \propto \gamma_0 \frac{\hbar A v}{2V}\hat{m} \times (\hat{s} \times \hat{m}). \tag{14}$$

To obtain above expression we considered a single electron incident into the metal-ferromagnet interface, when adding the contribution of all the electrons it is necessary to consider that their spins are not necessarily oriented along the same direction, and if there were no preferred orientation the individual contributions would cancel out in average and no net torque would be exerted to the Magnetization. For this reason is that nanopillar is built out of two magnetic layers, the first magnetic layer that electrons find upstream of their flow acts as a polarizer which aligns their magnetic

[8] The actual mechanism is more complicated because a reflected current has to be considered as well, moreover after entering the ferromagnet the spin of an individual electron does not align very quickly with the magnetization but rather precesses around it, nevertheless classical dephasing of the electrons oscillations cancels efficiently the spin current perpendicular to the magnetization direction, for details see Stiles and Zangwill (2002).

[9] This component cannot enter into LLG equation because of the restriction that the magnitude of $\mathbf{M}$ is constant.

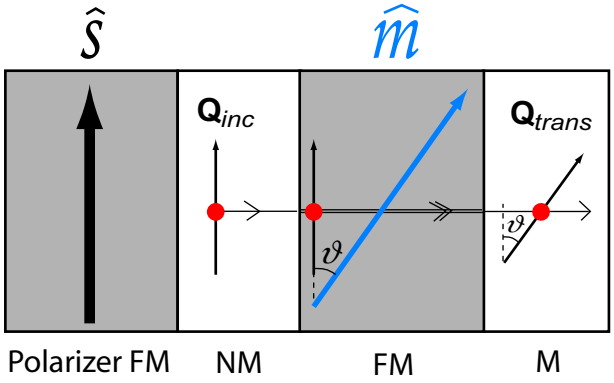

FIGURE 1.2. Schematics of the spin transfer mechanism.

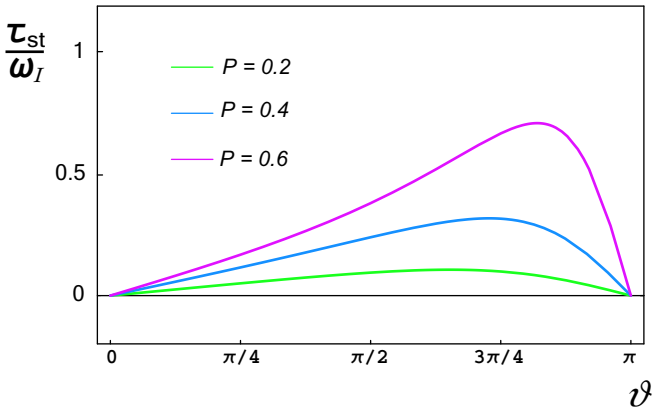

FIGURE 1.3. Slonczewski spin torque for different electron spin polarizations P.

moments along $\hat{s}$ (see Figure 1.2), then when encountering the second magnetic layer their magnetic moments are not collinear with the local magnetization and resulting in a total spin transfer torque given by

$$\mathbf{T}_{st} = \gamma_0 g(\hat{s}\cdot\hat{m};P)\frac{n\hbar A v}{2}\hat{m}\times(\hat{s}\times\hat{m}), \tag{15}$$

where n is the electron number density and the factor $g(\hat{s}\cdot\hat{m};P)$ gives the actual efficiency in the spin transfer (incorporating all the details about the electron spin dependent transport) at a given electron spin polarization P:

$$P = \frac{n_\uparrow - n_\downarrow}{n_\uparrow + n_\downarrow}, \tag{16}$$

where $\uparrow$ and $\downarrow$ designate the majority spin and minority spin electrons respectively. The function $g(\hat{s}\cdot\hat{m};P)$, usually referred to as g-factor or efficiency factor, is material and geometry dependent, it depends on the relative angle ϑ between the polarization direction of the incident electrons, $\hat{s}$, and the magnetization direction, $\hat{m}$. It is sometimes approximated by a constant, and the simplest functional form that incorporates the polarization P was found by Slonczweski in his original paper (Slonczewski, 1996):

$$g(\hat{s}\cdot\hat{m};P)=\frac{1}{f(P)(3+\hat{s}\cdot\hat{m})-4};\quad f(P)=\frac{(1+P)^3}{4P^{3/2}}. \tag{17}$$

Representative graphs of the strength of spin torque, $|\mathbf{T}_{st}|$, as a function of the angle ϑ are shown in figure Figure 1.3 for the Slonczewski form of the g-factor.

1.4. Metallic Nanopillars and Macrospin Model

Spin torque and spin dependent conductivity phenomena have been observed in different systems incorporating magnetic, metallic and insulating components. Many of the basic ideas so far discussed apply to several of these systems, but to further elaborate the theoretical considerations I will restrict to a more definite class of physical systems referred to as metallic nanopillar devices [10].

A metallic nanopillar device consists of thin magnetic layer of a soft ferromagnetic material named free layer typically made of $Ni_{80+\delta}Fe_{20-\delta}$ (permalloy) or $Co_{90+\delta}Fe_{10-\delta}$ which has therefore a low coercivity and thus its magnetization is easy to reorient and a fixed or pinned layer with a high coercivity so that its orientation change is negligible [11] and serves as the polarizer layer.

The free layer is typically patterned elliptical to produce a preferred axis of orientation for the magnetization, its width is around 100nm and thickness around 5nm. Even though the current perpendicular to plane (CPP) configuration is customarily used because of its higher magnetoresistance values, in plane configurations are also possible. The available techniques for measuring the magnetization dynamics are rather limited and most of them rely in the giant magnetoresistance effect (GMR) (Baibich et al., 1988; Binasch et al., 1989), which is the dependence of the resistance of a multilayer sandwich on the relative orientation of the magnetization of each ferromagnetic layer, in particular for the nanopillar shown in fig. Figure 1.1 the resistance is minimal for parallel magnetizations and maximal for antiparallel magnetizations.

A continous description of the dynamics of a metallic nanopillar like the ones previouly described would combine the LLG equation with the spin torque (9), even

[10] Some of the results I will derive can be applied to moderately modified versions of the metallic nanopillar, like magnetic tunnel junctions and nonlocal spin valves

[11] This is typically achieved by making the fixed layer much thicker than the free layer, by exchange biasing the layer with an extra antiferromagnetic layer or by making it much wider than free layer (extended layer) (see eg. Krivorotov et al. (2005); Garzon et al. (2008))

though this description accurately incorporates a wide variety of dynamical regimes observed in experiments, it is very diffucult to approach with analytical methods and in a broad range of measurements that level of detail is not required. This picture can be extraordinarily simplified if the magnetization of the ferromagnetic layers is considered as spatially uniform, leaving then its orientation as the only degree of freedom which enters into the LLG equation. This approximation is typically valid as long as the nanopillar is sufficiently small and the exchange interaction sufficiently high so as to strongly penalize any small deviations from uniform magnetization [12].

Under this approximation we can therefore write the magnetization of the free layer as $\mathbf{M}(\mathbf{r}, t) = M\hat{m}(t)$. The energy functional (1) and the effective field (3) are greatly simplified under this assumption.

In the first place the energy associated with the external magnetic field and the crystalline anisotropy of the ferromagnet can be simply written as

$$E(\hat{m}) = -\mu_0 MV(\mathbf{H}_{ext} \cdot \hat{m}) - K_a V(\hat{a} \cdot \hat{m})^2. \tag{18}$$

The energy associated with the dipolar field gives rise to the so-called demagnetization fields, this energy is determined by the geometry of the sample and in general from equation (1) can be seen to be a bilinear form of the magnetization $\mathbf{M}$

$$E_{demag}(\hat{m}) = \frac{\mu_0}{2} VM^2 \sum_{ij} n_{ij} m_i m_j, \tag{19}$$

The components of the demagnetization tensor n_{ij} are in the notation of equation (1) given by

$$n_{ij} = -\frac{1}{4\pi V} \int d^3r \int d^3r' \left(\frac{x_i x_j}{|\mathbf{x}|^5} \right), \tag{20}$$

[12]For a detailed study of deviations from the macrospin picture and the computed assisted simulations of nanopillars see Berkov and Miltat (2008)

where an irrelevant term proportional M^2 has been already omitted. We will not concern ourselves into computing the exact form of the demagnetization tensor in terms of the geometric parameters of a nanopillar (the derivation for an ellipsoid can be found in Landau and Lifshitz (1984)). For the thin planar elliptical nanopillar typically two terms appear, one usually called easy plane anisotropy which incorporates the fact that orientations out of the plane are less favorable energetically, and the second one, the easy axis anisotropy expresses the preference of the magnetization to lie parallel to the long axis of the ellipse. With this the anisotropic demagnetization energy can be written as [13]

$$E_{demag}(\hat{m}) = \frac{\mu_0}{2} V M^2 (\hat{m} \cdot \hat{p})^2 - \frac{\mu_0}{2} V M H_K (\hat{m} \cdot \hat{a})^2, \tag{21}$$

with $\hat{p}$ the unit vector normal to the easy plane of the nanopillar and $\hat{a}$ the vector along the easy axis. Generally this axis is chosen to coincide with one of the crystalline axis of the ferromagnet [14], in this case the easy axis anisotropy field strength H_K [15] can be thought as containing both, contributions from shape and intrinsic anisotropy, then we can write the total magnetic energy of the nanopillar as,

$$E(\hat{m}) = \frac{\mu_0}{2} V M^2 (\hat{m} \cdot \hat{p})^2 - \frac{\mu_0}{2} V M H_K (\hat{m} \cdot \hat{a})^2 - \mu_0 M V (\mathbf{H}_{ext} \cdot \hat{m}). \tag{22}$$

It is worth mentioning that the external magnetic field may contain not only the externally applied magnetic field to the free layer of the nanopillar but also any field coming from the dipolar coupling with the fixed layer or even terms that are not strictly speaking magnetic fields but that have the same functional form in the

[13] The easy plane anisotropy can be easily shown to have this form for an infinitesimally thin nanopillar using the notion of solid angle of a surface $\Omega = \int_S \frac{\hat{x} \cdot \hat{n}}{|x|^2} da$.

[14] The crystalline anisotropy is typically much smaller than the demagnetization anisotropy associated to the shape of the sample for typicall metallic ferromagnets.

[15] H_K is defined as the strength of the critical magnetic field required to produce magnetic switching when applied in the direction of the easy axis of the nanopillar and usually referred to as Stoner-Wolfarth switching field.

contribution to the magnetic energy like the exchange coupling between the fixed layer and the free layer through the intermediate metallic spacer [16].

The effective magnetic field can then be computed by the anologue to equation (2), where now the derivative with respect the magnetic moment $\boldsymbol{\mu} = V\boldsymbol{M}$ needs to be computed, in this case the effective field can be found from

$$\mathbf{H}_{eff}(\hat{m}) = -\frac{1}{\mu_0 V M}\frac{\partial E}{\partial \hat{m}}, \tag{23}$$

thus from equation (22), the effective field is

$$\mathbf{H}_{eff}(\hat{m}) = -M\hat{p}(\hat{p}\cdot\hat{m}) + H_K\hat{a}(\hat{a}\cdot\hat{m}) + \mathbf{H}_{ext}. \tag{24}$$

On the other equation (9) can be written in this case as

$$\frac{d\hat{m}}{dt} = -\gamma_0\mu_0\hat{m}\times\mathbf{H}_{eff} + \alpha\hat{m}\times\frac{d\hat{m}}{dt} + \frac{1}{MV}\mathbf{T}_{st}, \tag{25}$$

by replacing the explicit form of $\mathbf{T}_{st}$ from eq. (15) we obtain the LLG equation for the magnetization direction of a single domain nanopillar under the influence of spin torque,

$$\frac{d\hat{m}}{dt} = \mathbf{h}_{eff}\times\hat{m} + \alpha\hat{m}\times\frac{d\hat{m}}{dt} + \omega_I g(\hat{m}\cdot\hat{s})\hat{m}\times(\hat{s}\times\hat{m}), \tag{26}$$

where $\mathbf{h}_{eff} = \gamma_0\mu_0\mathbf{H}_{eff}$ explicitly reads as:

$$\mathbf{h}_{eff} = \omega_a\hat{a}(\hat{m}\cdot\hat{a}) - \omega_p\hat{p}(\hat{m}\cdot\hat{p}) + \omega_H\hat{h}, \tag{27}$$

where $\hat{h}$ is the unit vector along the external magnetic field $\mathbf{H}_{ext}$. All the ω's constants have units of frequency and can be explicitly related to the previously introduced constants by:

[16]Exchange coupling is an interaction between the magnetizations of different layers in multilayers stacks which originates in the spin dependent "trapping" of the electrons in the intermediate non-magnetic spacers which has a form $J_{ex}\hat{s}\cdot\hat{m}$, where the sign of J_{ex} has oscillatory behavior with the spacer thickness (see eg. Parkin et al. (1990); Bruno and Chappert (1991)).

$$\omega_p = \gamma_0 \mu_0 M,\ \omega_a = \gamma_0 \mu_0 H_K,\ \omega_H = \gamma_0 \mu_0 H_{ext},\ \omega_I = \gamma_0 \frac{\hbar j A}{2MVe}, \tag{28}$$

where $j = nev$ is the electric current density [17]. The fact that all the constants in the LLG equation (27) have units of frequency makes straightforward the comparison between strength of terms with different origins [18].

Equation (27) will be the starting point of the rest of work where we will address the question of how the dynamics of the magnetization of the free layer of a sufficiently small nanopillar is modified in the presence of the spin transfer torque.

[17] Strictly speaking j is minus the electric current density and is positive when the electrons flow from the fixed to the free layer

[18] In Gaussian units these constants are: $\omega_p = \gamma 4\pi M$, $\omega_a = \gamma H_K$, $\omega_H = \gamma H$ and $\omega_I = \gamma \frac{\hbar j A}{2MVe}$; the gyromagnetic ratio in gaussian units γ is related to that in SI units by $\gamma = c\gamma_0$.

Chapter 2

Spin Transfer Induced Switching

2.1. Linear Stability Analisis and Magnetization Switching

Equation (27) describes the variation of a unit vector $\hat{m}$ along the magnetization of the free layer of a nanopillar, therefore, its associated configuration space is the unit bidimensional sphere S^2. In the present work we will restrict to cases for which the parameters in this equation do not change with time, this precludes the possibility of chaotic dynamics (Bonin et al., 2007). The consistency of this fact is ensured by the condition

$$\hat{m} \cdot \frac{d\hat{m}}{dt} = 0, \tag{29}$$

which implies that the norm of the vector $\hat{m}$ is preserved by the dynamics. By taking the cross product of LLG equation (27) with $\hat{m}$ on both sides we can rewrite it as follows,

$$(1 + \alpha^2) \, \frac{d\hat{m}}{dt} = \mathbf{F}(\hat{m}) \equiv \boldsymbol{\tau}(\hat{m}) + \alpha \hat{m} \times \boldsymbol{\tau}(\hat{m}) \ , \tag{30}$$

where $\boldsymbol{\tau}$ is the sum of the torques coming from the effective magnetic field (which we call conservative torque $\boldsymbol{\tau}_c$) and the spin torque (which we call $\boldsymbol{\tau}_{st}$)

$$\boldsymbol{\tau} = \boldsymbol{\tau}_c + \boldsymbol{\tau}_{st}. \tag{31}$$

The factor $(1 + \alpha^2)$ in equation (30) can be eliminated by rescaling time $t' = t/(1 + \alpha^2)$, rendering this equation to the simple form [1]

[1] we will drope the prime from t' in all the remaining discussion

$$\frac{d\hat{m}}{dt} = \mathbf{F}(\hat{m}). \tag{32}$$

Above equation shows that the dynamics is completely contained in the way the vector field $\mathbf{F}$ flows around the unit sphere with the restriction $\mathbf{F} \cdot \hat{m}$, the fact that it is a first order differential equation eliminates the possibility of any "inertia", with the local velocity uniquely specified by the position itself. In the absence of damping ($\alpha = 0$) and spin torque ($\omega_I = 0$) the dynamics is conservative with the conserved quantity being the energy rescaled as follows

$$\varepsilon(\hat{m}) = \frac{\gamma_0}{\mu_0 V M^2} E(\hat{m}), \tag{33}$$

to which the effective field and conservative torque are related as

$$\mathbf{h}_{eff} = -\frac{\partial \varepsilon}{\partial \hat{m}}, \quad \boldsymbol{\tau}_c = \mathbf{h}_{eff} \times \hat{m}. \tag{34}$$

The fact that $\varepsilon(\hat{m})$ is conserved [2] specifies uniquely the trajectory, which can then be thought as the intersection of two surfaces, namely $\varepsilon(\hat{m}) = \varepsilon_0$ and $\hat{m}^2 = 1$. These orbits describe the precession of $\hat{m}$ around the local effective magnetic field (for an illustration see Figure 2.1). When damping is introduced the energy reduces with time and the magnetization spirals down to directions which minize it. Energy minima are therefore the only stable stationary solutions for the LLG equation under this condition. This situation can be dramatically altered with the introduction of spin torque which is able to stabilize equilibria otherwise corresponding to energy maxima and also precession cycles may become stable dynamical attractors (Bonin et al., 2007).

Even though exact dynamical solutions for equation (32) may be found for non-trivial but highly symmetric energy functions (see e.g. Sukhov and Berakdar (2009)),

[2] This is a direct consequence of $\frac{\partial \varepsilon}{\partial \hat{m}} \cdot \frac{d\hat{m}}{dt} = 0$

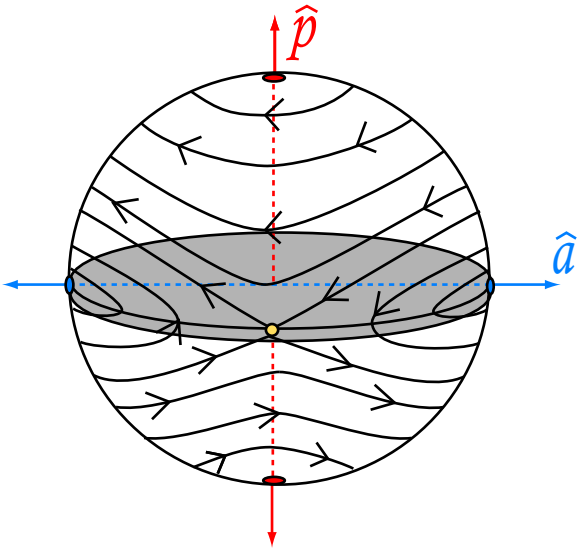

FIGURE 2.1. Schematics of constant energy trajectories for a typical nanopillar in the absence of external magnetic field

it is generally a difficult task and that degree of detail is seldom necessary. For memory applications mainly the knowledge of stable stationary magnetic configurations is needed [3] and this can be gained by linear stability analysis. Linear stability analysis usually proceeds by finding the equilibrium orientations, $\hat{m}_0$, as functions of the controllable parameters, which in typical experiments are the external magnetic field, ω_H, and the current, ω_I, these equilibria correspond to the zeroes of $\mathbf{F}$

$$\hat{m}_0(\omega_I, \omega_H) \quad : \quad \mathbf{F}(\hat{m}_0) = 0. \tag{35}$$

Equation (32) is then linearized around a given equilibria to find its local stability behavior. To do so it is convenient to choose a particular system of coordinates [4]. In spherical coordinates (ϕ, θ), the components of equation (32) along the unit vectors $\mathbf{e}_\phi$, $\mathbf{e}_\theta$ read as

$$\dot{\phi} \ \sin\theta = F^\phi(\phi, \theta), \qquad \dot{\theta} = F^\theta(\phi, \theta), \tag{36}$$

[3]Stable oscillatory solutions are important for other kinds of applications such as nanoscale microwave voltage generators, but we will not consider those dynamical regimes in the present work.

[4]This can be done also in a coordinate free language by introducing the tensor of covariant derivatives.

TABLE 2.1. Equilibria classification for the LLG equation

	$\mathrm{Tr}\hat{D} < 0$	$\mathrm{Tr}\hat{D} > 0$
$\det \hat{D} > 0$	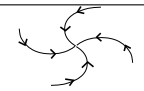	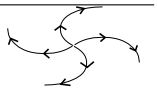
$\det \hat{D} < 0$	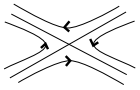	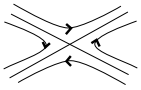

the linearized LLG equation can then be written in matrix form as [5]

$$\begin{pmatrix} \dot{\delta\phi} \\ \dot{\delta\theta} \end{pmatrix} = \begin{pmatrix} \frac{1}{\sin\theta}\frac{\partial F^{\phi}}{\partial \phi} & \frac{1}{\sin\theta}\frac{\partial F^{\phi}}{\partial \theta} \\ \frac{\partial F^{\theta}}{\partial \phi} & \frac{\partial F^{\theta}}{\partial \theta} \end{pmatrix}_{(\phi_0,\theta_0)} \begin{pmatrix} \delta\phi \\ \delta\theta \end{pmatrix} = \hat{D} \begin{pmatrix} \delta\phi \\ \delta\theta \end{pmatrix}, \tag{37}$$

where $\delta\phi \equiv \phi - \phi_0$, $\delta\theta \equiv \theta - \theta_0$ are infinitesimal deviations from the equilibria coordinates (ϕ_0, θ_0). The stability matrix $\hat{D}$ contains the information about the local dynamical behavior surrounding a given equilibrium. In particular the eigenvalues of this matrix given by

$$\lambda_{1,2} = \frac{\mathrm{Tr}\hat{D} \pm \sqrt{(\mathrm{Tr}\hat{D})^2 - 4\det \hat{D}}}{2}, \tag{38}$$

determine the stability nature. If the real part of both $\lambda_{1,2}$ is negative the equilibrium would be stable and if the real part of any of them is positive it would be unstable. From equation (38) this condition may be translated in terms of $\mathrm{Tr}\hat{D}$ and $\det \hat{D}$. For an equilibrium to be stable the requirements are

$$\mathrm{Tr}\hat{D}(\mathbf{n}_{eq}) < 0, \quad \det \hat{D}(\mathbf{n}_{eq}) > 0. \tag{39}$$

In fact the equilibria may be classified into stable and unstable centers and saddles (always unstable) as shown in Table 2.1. From a mathematical standpoint the task is then clear: find the position of an equilibrium as function of the parameters (ω_H, ω_I) from equation (35), in particular infer the existence region of the equilibrium in the

[5] We are assuming the equilibrium of interest not to lie on a singular point of the spherical coordinates, that is the north or south poles, in such case we may circumvent the problem by simply choosing another system of coordinates well defined at those points.

parameter space, evaluate then $\mathrm{Tr}\hat{D}$ and $\det \hat{D}$ in this region and delimit the sub-region for which conditions (39) are satisfied, this is the region at which the given equilibrium is stable. At the boundaries of this region the stability disappear and the given magnetic configuration then switches to another stable configuration [6], for some illustrative examples of this analysis see Bazaliy et al. (2004); Morise and Nakamura (2005).

Of particular interest is the value of the critical current at this boundary for a fixed magnetic field $\omega_{Ic}(\omega_H)$, this is the so called switching current and gives the critical current required to switch the magnetization of the nanopillar by means of spin transfer torques. Reducing this current without reducing the intrinsic magnetic stability of a given equilibrium [7] is one of the central challenges of the current memory oriented research in spintronics. Understanding the efficiency of spin transfer torque to produce switching constitutes then an important asset in this endeavour. The following section elaborates further on this idea of the efficiency of spin transfer to produce current induced switching, proposing a quantity that measures the ability of spin torque to produce this switching.

[6] In the case for which no stable equilibrium exists in some region of the parameter space necessarily stable precession cycles must exist.

[7] A physical device able to represent a classical bit of information must have at least two equilibrium configurations with a degree of stability as to support thermal fluctuations (so that memory is kept) that can be switched between this two in a controllable manner (so that the writing process is reliable).

2.2. Invariant Form of Spin Transfer Switching Condition

Further insight about the stability conditions (39) and current induced switching can be gained by analyzing them in terms of differential geometric quantities. In particular consider the divergence of the field $\mathbf{F}(\hat{m})$ in the sphere, which in spherical coordinates explicitly reads as

$$\nabla \cdot \mathbf{F} = \frac{1}{\sin\theta}\left(\frac{\partial}{\partial\theta}(\sin\theta F^{\theta}) + \frac{\partial F^{\phi}}{\partial\phi}\right) , \tag{40}$$

where ∇ is the gradient operator in the bidimensional unit sphere. From the form of the stability matrix $\hat{D}$ in equation (37) it is easy to verify that at any equilibrium point the following equality holds

$$\nabla \cdot \mathbf{F} = \mathrm{Tr}\hat{D}, \tag{41}$$

even though $\nabla \cdot \mathbf{F}$ and $\mathrm{Tr}\hat{D}$ are in general different functions.

Therefore $\nabla \cdot \mathbf{F}$ can replace $\mathrm{Tr}\hat{D}$ in the first inequality in (39). The $\nabla \cdot \mathbf{F} < 0$ stability condition gets then a straightforward geometric interpretation when expressed in integral form by means of Gauss theorem. Consider an arbitrary small closed contour Γ in the unit sphere surrounding a given equilibrium, the line integral of the normal component of $\mathbf{F}$ normal to the contour is related to the area integral of $\nabla \cdot \mathbf{F}$ in the region inside the contour, A, as follows (Arfken, 1995)

$$\oint_{\Gamma} \mathbf{F} \cdot \mathbf{e}_{\perp}\, dl = \int_{A} \nabla \cdot \mathbf{F}\, dA, \tag{42}$$

where $\mathbf{e}_{\perp}$ is the unit vector outward normal to Γ, and A is the area inside the contour. Therefore $\mathrm{Tr}\hat{D} < 0$, can be expressed as the condition that the average component of $\mathbf{F}$ normal to any small contour around an equilibria is negative [8]

[8] This condition rests in the assumption of a continuous variation of div$\mathbf{F}$ in the vicinity of the given equilibria.

$$\langle \mathbf{F} \cdot \mathbf{e}_{\perp} \rangle_{\Gamma} < 0, \tag{43}$$

in other words this condition is simply the requirement for the torque $\mathbf{F}$ to push inwards in average at the vicinity of a stable equilibrium.

Let us now find $\nabla \cdot \mathbf{F}$ using the explicit form of $\mathbf{F}$. From equation (30) we find

$$\nabla \cdot \mathbf{F} = \nabla \cdot \boldsymbol{\tau} - \alpha \nabla \times \boldsymbol{\tau}, \tag{44}$$

where $\nabla \times \boldsymbol{\tau}$ is a pseudoscalar quantity [9] given by

$$\nabla \times \boldsymbol{\tau} \equiv -\frac{1}{\sin\theta}\left[\frac{\partial \tau_{\theta}}{\partial \phi} - \frac{\partial}{\partial \theta}(\sin\theta \tau_{\phi})\right]. \tag{45}$$

Equation (44) suggests that a Helmholtz decomposition of the vector field $\boldsymbol{\tau}$ is desirable. In such decomposition the divergenceless component of $\boldsymbol{\tau}$ would be the one that affects $\nabla \cdot \mathbf{F}$ from pure damping origin whereas the irrotational component would appear as a direct modification of $\nabla \cdot \mathbf{F}$. Fortunately the conservative torque, $\boldsymbol{\tau}_c$, and spin transfer torque, $\boldsymbol{\tau}_{st}$, are already a natural Helmholtz decomposition of $\boldsymbol{\tau}$ (see eq. (31)) [10]

$$\begin{aligned} \boldsymbol{\tau}_c &= -\nabla\varepsilon(\hat{m}) \times \hat{m}, \quad \nabla \cdot \boldsymbol{\tau}_c = 0 \\ \boldsymbol{\tau}_{st} &= \omega_I \; g(\hat{m}) \; [\hat{m} \times (\hat{s} \times \hat{m})], \quad \nabla \times \boldsymbol{\tau}_{st} = 0, \end{aligned} \tag{46}$$

with above equations we can then write equation (44) in the following way

$$\nabla \cdot \mathbf{F} = \nabla \cdot \boldsymbol{\tau}_{st} - \alpha \nabla \times \boldsymbol{\tau}_{\mathrm{c}} = \nabla \cdot \boldsymbol{\tau}_{\mathrm{st}} - \alpha \nabla^2 \varepsilon. \tag{47}$$

[9] The curl "$\nabla\times$" in a bidimensional space has a scalar character.

[10] That $\boldsymbol{\tau}_c$ is divergenceless is a direct consequence of it being conservative, the condition of $\boldsymbol{\tau}_{st}$ being irrotational is, nevertheless, not so natural and in fact related to the particular form of $\boldsymbol{\tau}_{st}$ in metallic nanopillars, indeed for other structures like magnetic tunnel junctions there is an non-irrotational component of the spin torque known as perpendicular spin torque, for a review on spin transfer torques in magnetic tunnel junctions see Sun and Ralph (2008).

Equation (47) contains important insights into the identification of a quantity that represents the ability of spin transfer torque to poduce magnetic switching, in the sense that we have explicitly separated out the quantity that determines wether an equilibrium is stable or not, that is $\nabla \cdot \mathbf{F}$, into a contribution that comes from the intrinsic free magnetic dynamics of the system, namely $-\alpha\nabla^2\varepsilon$, plus a contribution that depends only on the spin torque, that is $\nabla \cdot \boldsymbol{\tau}_{st}$.

To understand the limits on which $\nabla \cdot \boldsymbol{\tau}_{st}$ plays the role of switching efficiency of spin torque, and to further ellaborate into what this concept means, let us examine more carefully how the magnetic switching in nanopillars occurs. If we go back to Table 2.1 we can see that an originally stable magnetic configuration can be made unstable, and therefore produce switching, by either changing the sign of $\mathrm{Tr}\hat{D}$ (which is equal to $\nabla \cdot \mathbf{F}$ at the equilibrium) or the sign of $\det \hat{D}$. As mentioned in section 1.2 the dimensionless damping parameter is typically smaller than 1 ($\alpha \sim 0.01$), and therefore constitutes a naturally small parameter of the system. It can be proved [11] that the sign of the determinant, and therefore the critical current at which it becomes zero, is independent of α. On the contrary $\nabla \cdot \mathbf{F}$, and thus the critical current at which it becomes zero, explicitly depends on α. Moreover $\nabla^2\varepsilon$ would be of the order of the magnetic constants defined in equation (28) for any equilibrium, therefore equation (47) implies that the critical current at which $\nabla \cdot \mathbf{F}$ becomes zero, ω_{Ic}, is in general small as compared to the magnetic constants

$$\frac{\omega_{Ic}}{\omega} \sim \alpha. \tag{48}$$

where ω designates generically the magnetic constants. On the contrary the critical current associated with $\det \hat{D} = 0$ would generally be of the order of the magnetic constants [12]. Because of this situation, switching will be, for most cases, achieved by

[11] see section 2.3.

[12] A concrete illustration of this considerations will be given in section 3.1

changing the sign of $\nabla \cdot \mathbf{F}$ rather than that of $\det \hat{D}$ [13], in this sense the tendency of spin torque to stabilize or destabilize a given equilibrium can be associated with the tendency of it to make $\nabla \cdot \mathbf{F}$ negative or positive and in particular the critical current, ω_{Ic}, would be that for which $\nabla \cdot \mathbf{F}\big|\omega_{Ic} = 0$.

Strictly speaking, spin torque affects $\nabla \cdot \mathbf{F}$ not only directly via $\nabla \cdot \boldsymbol{\tau}_{st}$ but it also indirectly modifies the term $-\alpha\nabla^2\varepsilon(\hat{m})$ in equation (47), because it changes the position of the equilibrium, $\hat{m}$, as a function of the current. Nevertheless because the critical currents are of first order in α (equation (48)), the shifting of the equilibrium points induced by spin torque would be of first order in α as well

$$\hat{m}_{eq}(\omega_{Ic}) = \hat{m}_{eq}(0) + \Delta\hat{m}_{eq}, \quad \Delta\hat{m}_{eq} \propto \omega_{Ic} \propto \alpha, \tag{49}$$

therefore the contribution to $\nabla \cdot \mathbf{F}$ coming from the equilibrium shifting induced by spin torque is of order α^2, and can reasonably be neglected. In this regime it is therefore legitimate to associate the spin torque induced modification of $\nabla \cdot \mathbf{F}$ with $\nabla \cdot \boldsymbol{\tau}_{st}$, and this quantity can be confidently identified with spin torque switching ability. Moreover a simplified version of the stability condition can be written,

$$\nabla \cdot \boldsymbol{\tau}_{st}\big|_{\hat{m}(0)} \leq \alpha\nabla^2\varepsilon\big|_{\hat{m}(0)} + \mathcal{O}(\alpha^2), \tag{50}$$

where $\hat{m}(0)$ is the zero current orientation of the equilibrium in consideration, with equality achieved at the critical switching current. Importantly, all quantities in (50) are evaluated at the unperturbed equilibrium point $\hat{m}(0)$. In comparison, using expression (39) one needs to perform an explicit calculation of $\hat{m}_{eq}(\omega_{Ic})$ even in the first order expansion in α (see e.g. Bazaliy et al. (2004); Sodemann and Bazaliy (2009)). This welcome simplification is possible because $\nabla \cdot \mathbf{F}$ and $\mathrm{Tr}\hat{D}$ are different functions coinciding only at equilibrium points, and $\nabla \cdot \mathbf{F}$ proves to be a more convenient discriminator. Additional simplification is provided by the fact that the left hand side

[13] This situation is not absolutely precluded and will be one of the central issues considered in section 2.3.

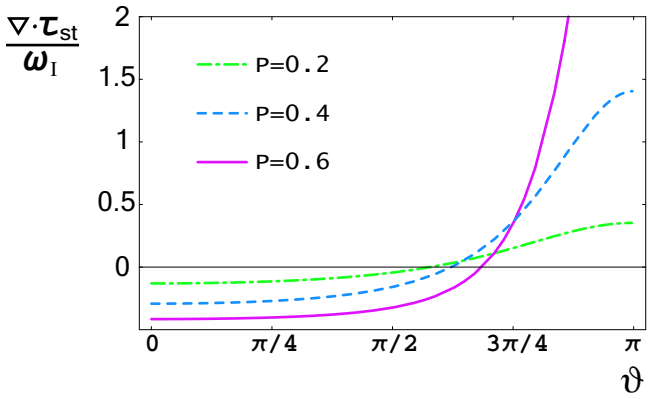

FIGURE 2.2. Divergence of spin torque for different electron spin polarizations P.

of (50) depends only on the properties of spin-transfer torque, i.e., on the efficiency function $g(\hat{m})$ and the polarizer direction $\hat{s}$, and the right hand side only depends on the form of magnetic energy ε.

Unlike the criteria (39), Eq. (50) operates with invariant quantities which can be evaluated in any coordinate system. From the explicit functional form of $\boldsymbol{\tau}_{st}$ given by equation (46) one gets

$$\nabla \cdot \boldsymbol{\tau}_{st} = -\frac{\omega_I}{\sin\vartheta}\frac{d}{d\vartheta}\big(g(\cos\vartheta)\sin^2\vartheta\big). \tag{51}$$

where ϑ is the angle between $\hat{s}$ and $\hat{m}$. Representative graphs of $\nabla \cdot \boldsymbol{\tau}_{st}(\vartheta)$ are shown in Figure 2.2 for the Slonczewski form of the efficiency factor $g(\vartheta)$ (equation (17)) at different spin polarizations P (equation (16)).

Some general remarks about the efficiency function, $\nabla \cdot \boldsymbol{\tau}_{st}$, are in order:

(a) Divergence $\nabla\cdot\boldsymbol{\tau}_{st}$ is not proportional to $|\boldsymbol{\tau}_{st}|$, that is, the efficiency of the spin torque to produce switching should not determined by its local strength, in particular the destabilization of noncollinear equilibria with respect to $\hat{s}$, for which the strength is larger may actually require larger current. In particular, for Slonczewski's form of g the largest destabilization power is observed in the anti-parallel state of $\hat{m}$ with respect to $\hat{s}$ (see Figure 2.2).

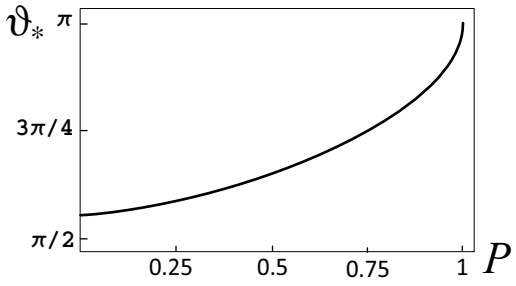

FIGURE 2.3. Critical angle as function of electron spin polarization P

(b) There exists a critical angle ϑ_* at which $\nabla \cdot \boldsymbol{\tau}_{st}(\vartheta_*) = 0$ (Figure Figure 2.2). For quilibrium points lying on the "critical circle" defined by $\vartheta(\phi, \theta) = \vartheta_*$ equation (50) predicts infinite critical current (more precisely, the linear in α approximation is violated and we can only state that the critical current will be large). The critical circle divides the unit sphere into two parts, so that for positive currents in one of them the spin-transfer torque tends to destabilize the energy minima and maxima while in the other it tends to make them more stable, and this tendency is reversed for negative currents.

(c) For a given form of $g(\vartheta, P)$ the critical angle ϑ_* is completely determined by the degree of spin polarization P from equation (51). The $\vartheta_*(P)$ dependence can be quite strong, as seen in the case of Slonczewski's g in Figure 2.3 where ϑ_* grows from a value slightly greater than $\pi/2$ at $P = 0$ to $\vartheta_* = \pi$ at $P \to 1$. In contrast, in the $g = \text{const}$ case $\vartheta_* = \pi/2$ is independent of P. Consequently the results of the stability calculation can strongly depend on the employed approximation of $g(\vartheta, P)$ whenever an equilibrium happens to be close to the critical circle.

The notion of the efficiency of spin torque will prove useful in chapter 3 where we will analyze specific configurations, with this idea seemingly anomalous stabilization regimes (see e.g. Bazaliy et al. (2004); Sodemann and Bazaliy (2009)) can be now intuitively understood. Moreover it opens the possibility of studying the stabilization

ability of non-standard functional forms of the spin torque like those recently proposed for antiferromagnetic nanopillars (Haney et al., 2008).

It is important to recognize that the low current assumption is necessary for $\nabla \cdot \boldsymbol{\tau}_{st}$ to meaningfully represent the switching ability, fortunately, this is the case for the typical critical currents. This switching is, nevertheless not fast, in the sense that it generally requires several precessional turns, each one typically of the order $100ps$, and during all this time the current is kept at the same constant value. Another approach is the so-called "ultrafast switching", in which high current pulses are applied in durations shorter than the typical precessional turns (Garzon et al., 2008), in this regime the local strength of the spin torque is understood to be the important quantity determining switching, rather than the divergence proposed in the present work. Even though it has been generally shown that the total energy required for switching is generally lower in the ultrafast regime, to produce the fast pulses in simple manners that could eventually be conveniently incorporated into memory devices remains challenging. Both approaches are therefore still significant candidates to be the switching mechanism in an eventually practical magnetic bit element.

2.3. Saddle Point Stabilization and Transcritical Bifurcations

The results obtained in the previous section relied on the idea that the quantity that determines switching in the limit of low damping was solely $\nabla \cdot \mathbf{F} = \mathrm{Tr}\hat{D}$, based on the assumption that the sign of the determinant is independent of the damping parameter α. In fact the following relation can be derived from equation (30)

$$\det \hat{D}_\alpha = (1+\alpha^2)\det \hat{D}_{\alpha=0} \equiv (1+\alpha^2)\det \hat{D}_{\boldsymbol{\tau}}, \tag{52}$$

which shows that α plays no role determining the change of sign in $\det \hat{D}$. Contrary to $\nabla \cdot \mathbf{F}$, $\det \hat{D}$ is not in general additive with respect to the addition of torques, this property was crucial in separating the contributions of the conservative and spin torques in $\nabla \cdot \mathbf{F}$. Nevertheless the following decomposition rule can be written at an equilibrium point in a special coordinate system where the polar angle ϑ is measured with respect to the polarizer direction $\hat{s}$ [14]

$$\det \hat{D}_{\boldsymbol{\tau}} = \det \hat{D}_{\boldsymbol{\tau}c} + \det \hat{D}_{\boldsymbol{\tau}st} - \frac{\partial \tau_c^\vartheta}{\partial \vartheta}\left(\frac{\partial \tau_{st}^\vartheta}{\partial \vartheta} - \frac{\cos\vartheta}{\sin\vartheta}\tau_{st}^\vartheta\right) \tag{53}$$

where the matrices $\hat{D}$ appearing in above equation correspond to the same definition given in equation (37) with the corresponding components of the specified vector field. This equation is not very illuminating in general except for particular cases when the last term vanishes and we can think of the determinant as being additive [15].

Since spin torque can stabilize and destabilize equilibria which at zero current correspond to maxima and minima of energy by changing the sign of $\nabla \cdot \mathbf{F}$ through its direct modification of $\nabla \cdot \boldsymbol{\tau}_{st}$, then, natural questions that arise are: can the spin

[14] It is necessary that this equilibrium point is not any of the singular points of the coordinate system

[15] Those will be considered later in this section in the contex of transcritical bifurcations.

torque stabilize equilibria which are saddle points at zero current?, and can spin torque destabilize energy minima or maxima by converting them into saddles [16]?.

At first glance the problem may seem very similar to the one already solved in the previous section, only that in this case we have to study when the function $\det \hat{D}_{\boldsymbol{\tau}}$ changes sign as the current is increased. Nevertheless, the fact that there is no generally a small parameter involved is reflected in the fact that equilibria will considerably shift their positions as the current is increased and therefore a proper identification of an efficiency function associated with the ability of spin torque to produce stabilization is in general not possible.

Other fundamental considerations make the problem of saddle point stabilization substantially different from that of maxima and minima. In particular centers [17] and saddles as zeroes of the vector field $\mathbf{F}$ differ in a characteristic topological property called winding number or Poincaré index. The Poincaré index associated with a saddle is -1 whereas for a center is 1. The Poincaré index theorem for the two dimensional sphere states that the sum of indices of all isolated fixed points equals 2. This theorem can be expressed in the following formula

$$N_C - N_S = 2, \tag{54}$$

where N_C and N_S are the total number of centers and saddles respectively. Poincaré index theorem poses restrictions in the stabilization of saddle points, and in general in processes that involve transformation of saddles into centers and vice versa. In particular if we consider the changes in the total number of centers, ΔN_C, and saddles, ΔN_S, resulting from changes in any parameter of the LLG equation, equation (54) leads to the restriction

$$\Delta N_C = \Delta N_S. \tag{55}$$

[16] In the case of energy maxima the question is whether they can be converted into saddles

[17] In the present context centers refer to sources or sinks of flow.

This restriction in particular prohibits the possibility of locally transforming an isolated saddle into an isolated center, that process would imply $\Delta N_S = -1$ and $\Delta N_C = 1$ in clear contradiction with this restriction [18]. Therefore it is necessary for an isolated saddle to become a center that other "distant" fixed points exchange their nature as well, and this is what we mean by non-local.

A possible scenario suggested by the restriction (55) is the saddle-center annihilation. This process is the one in which as the current is increased a saddle and a center approach each other merging at certain critical current and dissapearing as a consequence, in this process both the number of saddles and centers is decreased by 1, and therefore the condition (55) is satisfied [19]. It turns out that the saddle-center annihilation is in fact the most generic scenario and this bifurcation is robust (Crawford, 1991), in the sense that occurs for small pertubations in the configutarion of the device.

On the other hand, the non-local exchange of stability nature of two or more equilibria can occur but require special symmetry conditions that restrict their possible shiftings as the current is increased, these are normally discrete symmetries of the total torque under special transformations such as reflections or rotations [20]. This type of bifurcation is not robust in the sense that it is replaced by a merging type bifurcation when the configuration is slightly perturbed and the underlying symmetry is broken.

From above considerations it is clear that the saddle point stabilization problem is qualitatively different from that of centers (which correspond to energy minima and maxima at zero currents). Moreover the problem in general requires careful study of the shifting of equilibria as the current is increased, this makes it technically difficult,

[18]The reciprocal process is evidently prohibited as well.

[19]By the same argument the saddle-center creation is an allowed process as well, in such case the number of saddles an centers increases by 1.

[20]A particular illustration of these situations is given in section 3.2.

and unless simple forms of the spin torque and special symmetries are involved it is analytically untractable.

A particularly interesting type of bifucartion existing under special conditions is the transcritical bifurcation (Crawford, 1991). This appears in the case when the polarizer $\hat{s}$ coincides with an equilibrium $\hat{m}_0$ which is a saddle point at zero current. Therefore the spin torque is zero at this equilibrium and as the current increases the equilibrium remains "pinned" along the direction of the polarizer. In this situation we must consider equation equation (53) in the limit $\vartheta \to 0$ and the last term may be shown to vanish, leading to

$$\lim_{\vartheta \to 0} \det \hat{D}_{\boldsymbol{\tau}} = \det \hat{D}_{\boldsymbol{\tau} c}(\vartheta = 0) + \lim_{\vartheta \to 0} \det \hat{D}_{\boldsymbol{\tau} st}, \tag{56}$$

where $\hat{D}_{\boldsymbol{\tau} c}(\vartheta = 0)$ is basically the determinant of the stability matrix at the saddle point in the absence of spin torque which is necessarily negative (see Table 2.1), the determinant of the stability matrix associated with spin torque can be proven to be

$$\lim_{\vartheta \to 0} \det \hat{D}_{\boldsymbol{\tau} st} = (\omega_I g(\vartheta = 0, P))^2. \tag{57}$$

Therefore there is a critical current at which $\det \hat{D}_{\boldsymbol{\tau}} = 0$ and the saddle becomes a center given by

$$\omega_{Icrit} = \frac{\sqrt{-\det \hat{D}_{\boldsymbol{\tau}_c}(\vartheta = 0)}}{g(\vartheta = 0, P)}. \tag{58}$$

According to the previous discussions of the Poincaré index theorem this transformation cannot occur for an isolated saddle point. In the generic case what occurs is that a center approaches the saddle and at the critical current they "exchange" their stability nature in a collision-like process (see Figure 2.4(a)), which is the transcritical bifurcation itself (Crawford, 1991) [21]. When the position of the polarizer is

[21] What "generic" means in the present context is that there are no special symmetries restricting the approach of the center to the direction of the polarizer as the current increases, another "non-genreric" scenario is that more than one center approach the saddle as the current increases, these

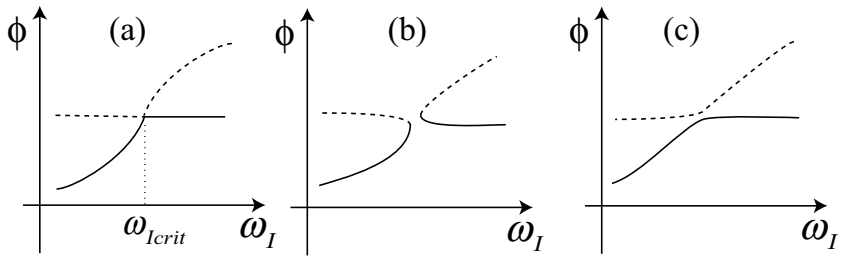

FIGURE 2.4. Current dependence of equilibrium position $\phi(\omega_I)$ for $\hat{s}$ directed exactly (a) or close (b,c) to the saddle point. Dashed lines show saddles, solid lines show centers.

slightly perturbed, the abrupt center saddle transformation is replaced by crossover in a small current interval. This is guaranteed by the fact that at low current the saddle point has to remain near $\hat{s}$ and at large current a stable equilibrium near $\hat{s}$ is inevitably produced by the increasing attraction of $\hat{m}$ to $\hat{s}$. The crossover can happen in two ways (see Figure 2.4(b,c)). Case (b) is a generic destruction and creation of the saddle-center pair. Case (c) is formally not a bifurcation, but looks like one for all practical purposes if the misalignment is small. It can be detected by an anomalously close approach of equilibria, which in this case is a truly better criteria then $\det \hat{D}_{\boldsymbol{\tau}} = 0$.

A particular illustration of the transcritical bifurcation will be given in section 3.2. Transcritical bifurcations have the importance that the critical current can be analytically predicted in general. To the best of our knowledge no such bifurcations have been studied in real devices, these bifurcations may be interesting in the context of the study of noise and fluctuation phenomena present in the nanopillar, because they may be expected to be magnified in the proximity of such bifurcations.

two cases will be illustrated for the spin flip transistor in section 3.2 and will correspond to zero and non-zero external magnetic field ω_H respectively.

Chapter 3

Selected Applications

3.1. Metallic Nanopillar with In-plane Magnetic Field

The spin transfer switching in metallic nanopillars with an external in-plane magnetic field perpendicular to the direction of the easy axis has been extensively studied both theoretically (see eg. Sun (2000); Smith et al. (2005); Sodemann and Bazaliy (2009)) and experimentally (see eg. Mancoff et al. (2003); Smith et al. (2005); Garzon et al. (2008)). The schematic representation of the device is shown in Figure 3.1. In this configuration the two easy axis directions, which we call parallel (P) and antiparallel configurations (AP), are the ones of main interest, they are the two states that would eventually codify a magnetic bit. This configuration is of interest because by applying an external magnetic field perpendicular to the easy axis of free layer these two equilibrium configurations can be brought closer, and therefore it is possible to study the switching behavior as a function of this "closeness", which is determined by the relative strength of the magnetic field with respect to the anisotropy field (see Figure 3.1). In particular, because the orientation of the polarizer $\hat{s}$ remains fixed as the field is increased this configuration results suitable to study the angle dependence of the switching efficiency of the spin torque.

To describe this configuration we choose the system of coordinates so that the polar axis coincides with the direction of the polarizer, which is the same of the easy axis, that is $\hat{s} = \hat{a} = \hat{e}_z$, $\hat{h} = \hat{e}_x$, $\hat{p} = \hat{e}_y$. The energy function, $\varepsilon(\hat{m})$, coming from equations (22) and (33) can be written as

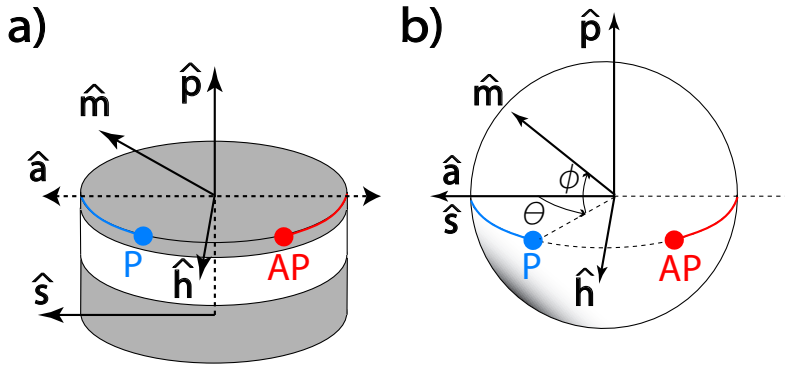

FIGURE 3.1. a) Typical nanopillar device. b) In plane magnetic field configuration.

$$\varepsilon(\hat{m}) = \frac{\omega_p}{2}(\hat{p}\cdot\hat{m})^2 - \frac{\omega_a}{2}(\hat{a}\cdot\hat{m})^2 - \omega_H(\hat{h}\cdot\hat{m}), \tag{59}$$

where the constants are the same defined in equation (28). The components of the torque $\boldsymbol{\tau}$, which includes the conservative torque and the spin torque, can then be computed in spherical coordinates

$$\begin{aligned}\tau_\phi &= \frac{1}{2}\sin 2\theta(\omega_p \sin^2\phi + \omega_a) - \omega_H \cos\theta\cos\phi,\\ \tau_\theta &= -\frac{\omega_p}{2}\sin\theta\sin 2\phi - \omega_H \sin\phi - \omega_I g(\theta, P)\sin\theta.\end{aligned} \tag{60}$$

The equilibirum configurations, which correspond to $\tau_\phi = \tau_\theta = 0$, can in principle be solved for any external field ω_H and current ω_I, but in practice this cannot be done analytically. Nevertheless the problem is greatly simplified in the case of zero current for which the positions of the P and AP configurations are

$$\sin\theta_{P,AP} = \frac{\omega_H}{\omega_a}, \qquad \sin\phi_{P,AP} = 0, \tag{61}$$

for $\omega_H < \omega_a$, which defines the range of fields of our interest.

The current induced shifting of this equilibria is normally negligible in this configuration. The main reason is that easy plane anisotropy torque is large compared to any other torque for the equilibria that lie in the nanopillar plane, in fact the easy

axis anisotropies and the typical magnetic fields used for these devices are about ∼10-50mT, on the other hand the easy plane anisotropy for very thin free layers (thickness of about $5nm$) are about ∼1-2T, this means that the easy plane anisotropy strength, ω_p, is about a hundred times larger than the easy axis anisotropy, ω_a. When the currents are turned on the spin torque will tend to shift equilibria out of the easy plane in the azimuthal direction at first order, but this effect is greatly suppresed by the strong easy plane anisotropy, as a consequence the first order spin torque induced shifting, in powers of ω_I/ω_p is

$$\sin\theta_{P,AP} = \frac{\omega_H}{\omega_a} + \mathcal{O}\left(\frac{\omega_I}{\omega_p}\right)^2, \qquad \sin\phi_{P,AP} = -g_{P,AP}\frac{\omega_I}{\omega_p}\left(1+\frac{\omega_a}{\omega_p}\right) + \mathcal{O}\left(\frac{\omega_I}{\omega_p}\right)^2. \quad (62)$$

Where $g_{P,AP} = g(\theta_{P,AP}, P)$. Because the applied field ω_H determines uniquely the polar angle orientation of the equilibria, θ, we will use them interchangeably in the rest of the discussion, therefore whenever θ appears in the rest of this section it must be understood that it is the polar orientation of the equilibria which is fixed by the external magnetic field. To determine the switching currents as a function of the field we use the ideas developed in section 2.2, according to which the sign of the divergence of the total torque, $\nabla \cdot \mathbf{F}$, determines whether an equilibrium is stable or not. before that, in order to illustrate that the determinant does not play a major role in determining the critical currents for switching between energy minima and maxima, let us compute it explicitly. From the definition of the stability matrix $\hat{D}$ from equation (37) we obtain

$$\frac{1}{1+\alpha^2}\det\mathbf{D} = \omega_a(\omega_p+\omega_a)\cos^2\theta + \mathcal{O}(\omega_I^2). \quad (63)$$

Therefore it is clear that it remains positive in the regime of our interest and does not affect switching. On the other hand the divergence is

$$\begin{aligned}\nabla \cdot \mathbf{F} = &- \omega_I(g(\theta)\cos\theta + \frac{d}{d\theta}(g(\theta, P)\sin\theta)) \\ &- \alpha(\omega_p \cos 2\phi + (\omega_p \sin^2\phi + \omega_a)(1 + \cos^2\theta)).\end{aligned} \tag{64}$$

The first term is the divergence of spin torque, but in this case the angle between the polarizer and the free layer polarization is simply the polar angle $\vartheta = \theta$ (see equation (51)). The second term is the curl of the conservative torque (compare with equation (47)). The condition of stability is reduced to the negativity of $\nabla \cdot \mathbf{F}$. To show how the divergence of spin torque can be used to quantify its switching ability let us contrast the stability behavior for two functional forms of the efficiency factor $g(\theta, P)$, namely the $g = const$ approximation and the Slonczewski form for g (see equation (17)).

For the g constant approximation the currents for which the P and the AP configurations are stable are given by

$$\omega_I \gtrless \mp\alpha \frac{\omega_p + \omega_a(2 - (\omega_H/\omega_a)^2)}{2g\sqrt{1 - (\omega_H/\omega_a)^2}} \tag{65}$$

where $>, -$ $(<, +)$ corresponds to the P (AP) stability region (See figure Figure 3.2d), with equality achieved at the critical switching current. The switching current is symmetric for switching from P to AP and AP to P (only difers by sign), and exhibits the $1/\cos\theta$ divergence reported in previous studies (Sun, 2000; Mancoff et al., 2003). For the Slonczewski g factor, the stability condition for P reads as,

$$\omega_I > -\alpha \frac{\omega_p + \omega_a(2 - (\omega_H/\omega_a)^2)}{2g_N\sqrt{1 - (\omega_H/\omega_a)^2} + g_N^2 f(\omega_H/\omega_a)^2}, \tag{66}$$

with equality achieved at the critical switching current. For the AP equilibrium we have

$$\omega_I \lesseqgtr \alpha \frac{\omega_p + \omega_a(2 - (\omega_H/\omega_a)^2)}{2g_S\sqrt{1 - (\omega_H/\omega_a)^2} - g_S^2 f(\omega_H/\omega_a)^2}, \tag{67}$$

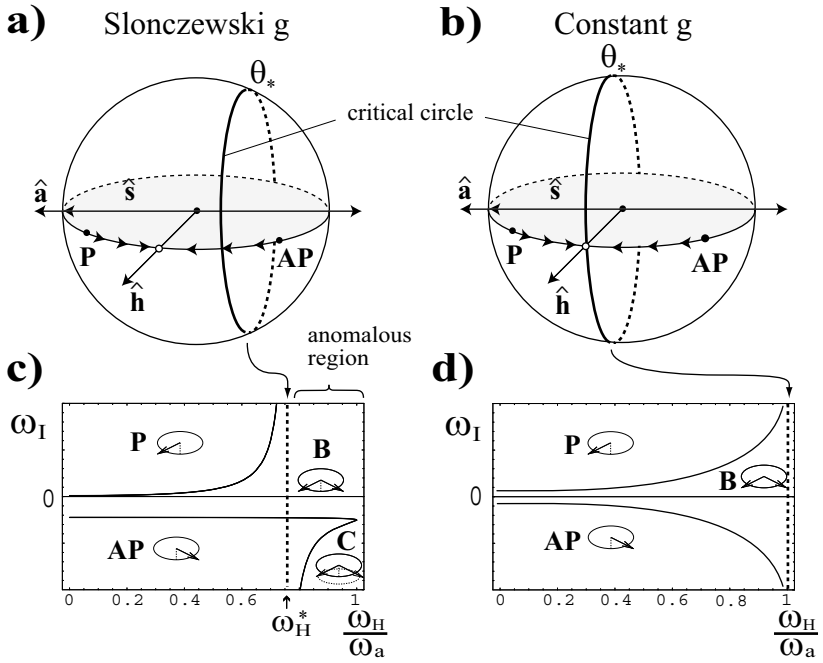

FIGURE 3.2. Stability diagram for $P = 0.7$, $\alpha = 0.01$, $\omega_a/\omega_p = 0.01$ (values of ω_I and ω_H are mesured relative to ω_p). Stable regions for P and AP states, bistable region B and precessional cycles C, in terms of the current ω_I and magnetic field ω_H ($\omega_H^*/\omega_a = 0.76$).

where $<$ ($>$) is the condition for $\omega < \omega_H^*$ ($\omega > \omega_H^*$), ω_H^* designates the field for which the denominator of equation (67) becomes zero. The stability diagram is shown in figure Figure 3.2c. The angle θ_* of the AP state that corresponds to the field ω_H^*, is nothing but the critical angle at which the divergence changes sign discussed in section 2.2, as mentioned before θ_* depends only the polarization and can be found to be

$$\cos\theta_c = -\sqrt{1-(\omega_H^*/\omega_a)^2} = \sqrt{\xi_P^2 - 1} - \xi_P. \tag{68}$$

It is easy to interpret the stability diagrams shown in figure Figure 3.2 when analyzed in terms of divergence. In the g constant case the divergence becomes zero at the critical angle $\theta_* = \pi/2$ (see fig Figure 3.2b), therefore in the vicinity of this region the switching efficiency is almost zero [1] and the required currents to produce

[1]The switching efficiency is the divergence, the switching currents will be inversely proportional to this efficiency.

switching diverge in the linear approximation, on the contrary for zero magnetic field $\omega_H = 0$, that is for $\theta = \{0, \pi\}$, the divergence is maximum and then the critical current is minimum. The symmetry of the switching diagram is naturally explained from the symmetry of the magnitude of the divergence about $\theta = \pi/2$.

For the slonczewski g factor we have the same qualitative behavior for $\omega_H < \omega_H^*$, except for the high asymmetry of the switching current, which is smaller for switching from AP to P than from P to AP at low magnetic fields, this comes from the high asymmetry of the divergence around $\theta = \pi/2$ as shown in Figure 2.2. As ω_H approaches ω_H^* the AP state approaches the critical angle θ_* at which the divergence vanishes and therefore the required switching current diverges. The seemingly anomalous switching behavior for $\omega_H > \omega_H^*$, in which AP is stable for positive currents and unstable for sufficiently large negative currents, is explained by the fact that the divergence has now the same sign that it has for the P configuration at a given field, therefore both P and AP tend to be stabilized for positive currents and destabilized for sufficiently large negative currents. An interesting region emerges in this regime where neither of the equilibria is stable suggesting the existence of an stable precession cycle (see Figure 3.2(c)).

Above discussion shows how the divergence of spin torque captures the essential features of a quantity representing its switching ability.

3.2. Spin Flip Transistor

The previous discussion has been focused on the spin transfer in nanopillar geometries, nevertheless some other devices can be analyzed within the same formalism of the spin torque and macrospin model. In this section we will discuss a planar device known as spin flip transistor (Bauer et al., 2001), which possesses three magnetic terminals, two of them, the source and drain, have fixed and antiparallel magnetizations, and the third terminal is made out of a soft magnetic material whose magnetization is able to rotate when a current induces spin transfer torque on it [2], this free layer is deposited on top of a normal metal as shown in Figure 3.3, and it is elliptically paterned as to provide two stable preferred orientations at zero current.

The switching behavior of the spin flip transistor has beeen previously studied theoretically (Wang et al., 2006; Bazaliy, 2007), and in fact the full stability diagram for constant g factor has been already found (Morise and Nakamura, 2005). Besides of the available understanding of the spin flip transistor switching, to the best of our knowledge, none of the present studies have underscored the underlying differences of this type of switching and stabilization, which is in fact a saddle point stabilization with a transcritical bifurcation as the ones discussed in section 2.3. This is so because the direction of the polarizers is chosen to coincide with the hard axis of the free layer, which is perpendicular to the easy axis equilibria orientations, this direction is a saddle point of magnetic energy and therefore the configuration meets the requirements for this kind of bifurcation to occur (see section 2.3).

[2]The spin transfer torque and magentoresistance do not require the current to be perpendicular to the plane of the device, as it is the case we are discussing in this section.

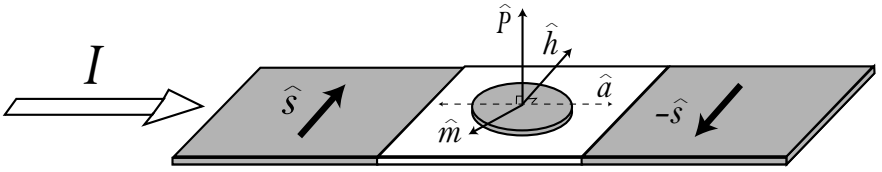

Figure 3.3. Spin flip transistor

Suppose that we apply an external magentic field in the direction of the hard axis [3]. Let us choose the system of coordinates $\hat{s} = \hat{h} = \hat{e}_z$, $\hat{p} = \hat{e}_x$, $\hat{a} = \hat{e}_y$, to describe the magnetization dynamics of the free layer. The components of $\boldsymbol{\tau}$ can be computed in the same way as in the previous section, and they read as

$$\begin{aligned} \tau_\phi &= \frac{1}{2}\sin 2\theta(\omega_p \cos^2\phi - \omega_a \sin^2\phi) + \omega_H \sin\theta, \\ \tau_\theta &= \frac{\omega_p + \omega_a}{2}\sin\theta \sin 2\phi - \omega_I g(\theta, P)\sin\theta. \end{aligned} \tag{69}$$

For simplicity we will assume a constant spin-transfer efficiency $g(\cos\theta) = g$ to study the stability behavior analytically, nevertheless, the conclusions here drawn are more general, and in particular apply for the Slonczewski form of the spin transfer efficiency as well. In this case the position of all the equilibrium points can be exactly computed for all values of current and magnetic field. The points $\theta = 0$ and $\theta = \pi$, which are the saddle points at zero magnetic field, are equilibria for any value of the current and magnetic field, we will denote them here as north (N) and south (S) poles. The azimuthal direction of the other equilibria can be found to be

$$\sin 2\phi = \frac{\omega_I g}{\frac{1}{2}(\omega_a + \omega_p)}, \tag{70}$$

for $|\omega_I| g < \frac{1}{2}(\omega_a + \omega_p)$, and the polar angle of the equilibria can be found to be [4]

$$\cos\theta = -\frac{\omega_H}{\frac{\omega_p - \omega_a}{2} - \sqrt{\left(\frac{\omega_p + \omega_a}{2}\right)^2 - (\omega_I g)^2}}, \tag{71}$$

The requirement $|\cos\theta| < 1$ determines the region of existence of these equilibria in terms of the current and magnetic field (ω_I and ω_H). The switching behavior in the zero magnetic field case, $\omega_H = 0$, is qualitatively different from that of the finite field

[3] That is the direction of the saddle point of our interest.

[4] We are not considering the equilibria corresponding to the extensions of the out of plane hard axis, which are energy maxima at zero current, because they do not play any role in the large easy plane anitropy regime.

case, the first one illustrates the case in which a nonlocal stabilization-destabilization of equilibria occur, whereas the second one illustrates the saddle point stabilization via transcritical bifurcations, these two possibilities were discussed in section 2.3 and they both are consistent with the restrictions imposed by the Poincaré index theorem.

In the $\omega_H = 0$ case the easy axis equilibria lie always in the plane perpendicular to the polarizer, defined by $\theta = \pi/2$, as can be inferred from equation (71), whereas their azimuthal orientation is given by

$$\cos 2\phi = -\sqrt{1 - \left(\frac{2\omega_i g}{\omega_a + \omega_p}\right)^2}, \tag{72}$$

It is clear therefore that saddles and easy axis never merge for any current. Now to be able to conclude that they undergo a non-local "exchange" of their stability nature it is necessary to compute the determinant of the stability matrix at both equilibria. In the case of the saddles (N,S) this can be obtained to be

$$\det \hat{D}_{N,S} = -\omega_a \omega_p + \omega_i^2 g^2, \tag{73}$$

This determinant becomes zero at a critical current

$$g\omega_{i-crit} = \sqrt{\omega_a \omega_p}, \tag{74}$$

For currents above this value N and S will be centers. Now in the case of the easy axis equilibria the determinant can be computed to be

$$\det \hat{D}_{axis} = (\omega_a + \omega_p)\cos 2\phi \left(\left(\frac{\omega_p - \omega_a}{2} \right) + \left(\frac{\omega_p + \omega_a}{2} \cos 2\phi \right) \right). \tag{75}$$

By replacing equation (72) in this determinant we find that the critical current at which it becomes zero turns out to be ω_{i-crit} obtained in equation (74), confirming that the saddle and the centers exchange their stability nature without approaching, exactly at this critical current in a way consistent with the Poincaré index theorem as discussed in section 2.3.

This nonlocal type of stabilization is nevertheless not robust, and the underlying reason for its existence is the inversion symmetry of the torque with respect to the plane perpendicular to $\hat{s}$. If this symmetry is slightly broken this abrupt exchange of local stability behavior is replaced by a merging. This is the case when a magnetic field pointing along $\hat{s}$ is introduced. In this case the position of the easy axis directions is given by equations (70) and (71). In particular from equation (71) we can see that as the current is increased the easy axis equilibria start approaching the saddle [5] and they merge with it for $\cos\theta = \pm 1$, thus the current and the field are related by

$$\omega_H = \pm \left(\sqrt{\left(\frac{\omega_a + \omega_p}{2} \right)^2 - (\omega_I g)^2} - \frac{\omega_p - \omega_a}{2} \right). \tag{76}$$

where the $+$ $(-)$ corresponds to merging with the N (S) saddle. On the other hand the determinant at the saddles (N and S) is given by

$$\det \hat{D} = -\left(\frac{\omega_p + \omega_a}{2} \right)^2 + \left(\left(\frac{\omega_p - \omega_a}{2} \right) \pm \omega_H \right)^2 + \omega_I^2 g^2, \tag{77}$$

where the $+$ $(-)$ corresponds to the N (S) saddle. Thus the critical current for which thes saddles become centers [6] is

$$\omega_{I crit} g = \sqrt{\left(\frac{\omega_p + \omega_a}{2} \right)^2 - \left(\left(\frac{\omega_p - \omega_a}{2} \right) \pm \omega_H \right)^2}, \tag{78}$$

which is the same current at which the centers merge with saddle obtained from equation (76).

This is a transcritical bifurcation with an extra special feature, namely the fact that two equilibria "collide" with the saddle at the same time leaving only a center afterwards. This feature of the bifurcation is not robust and emerges from another underlying symmetry of the torque, in this case the rotation by $\pi/2$ around $\hat{s}$ which is not broken by the introduction of a magentic field. When this symmetry is slightly

[5] For positive magnetic field they approach N ($\hat{s}$) and for negative ones they approach S ($-\hat{s}$).

[6] They both become centers at the same time

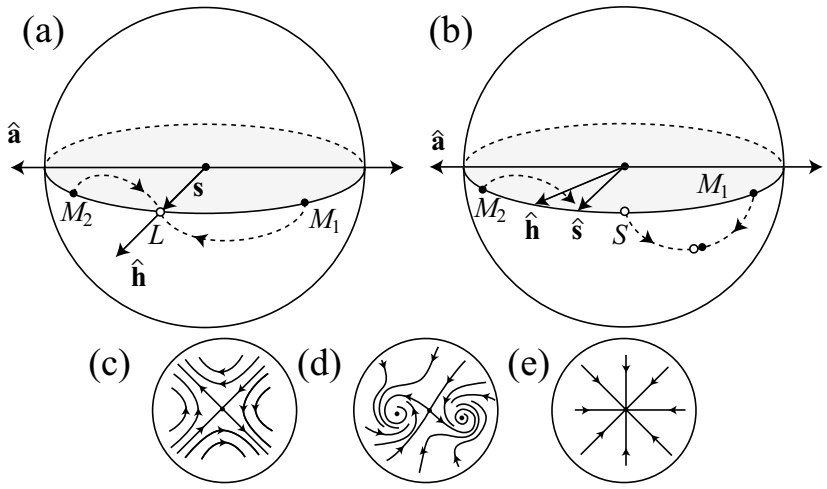

FIGURE 3.4. Transcritical bifurcation in the spin flip transistor. (a) The dashed lines show how the positions of the easy axis equilibria ($M_{1,2}$) approach the saddle, S, with increasing current and merge with it at a critical value given by eq. (78). (b) In-plane directions of $\hat{s}$ and $\hat{h}$ that slightly break the $\pi/2$ rotation symmetry. The saddle merges with one of the centers, while the other one asymptotically approaches $\hat{s}$. (c-e) transformation of the field $\mathbf{F}$ during the merger of the saddle with two centers in case (a).

broken the bifurcation is replaced by the "generic" case in which the saddle merges with a single one of the approaching centers. Figure 3.4 sketches the situation of this transcritical bifurcation, and how it is replaced when the symmetry is slightly broken.

Chapter 4

Summary and Conclusions

In the present work we have theoretically studied the stability properties of the magnetization of a single domain ferromagnetic layer in the presence of an external magnetic field, magnetic anisotropies and spin transfer torque.

By incorporating differential geometric quantities into the standard linear stability analysis we have singled out a function that represents the ability of spin torque to stabilize/destabilize equilibrium configurations corresponding to minima and maxima of magnetic energy. This quantity is the divergence of spin torque, explicitly presented in equation (51).

The meaning of this observation could be summarized in the following paragraph: The free dynamics of the magnetization vector is divergenceless, that is, the effective magnetic torques only produce precession around the energy minima and maxima; when damping is introduced this behavior is modified, precession is then accompanied by a spiraling motion into those orientations that minize the energy of the system, this is a consequence of the damping torque having a finite divergence, which is nevertheless small due to the smallness of the damping parameter α. When spin torque is introduced the divergence map of the total torque can be dramatically modified, due to the fact that spin torque is irrotational and therefore it only modifies the divergenceful part of the total torque, that is the damping torque, which is otherwise small due to the smallness of α. Consequently the local damping divergence can be compensated and in some cases canceled by the divergence of spin torque, leading to spin torque induced switching. This competition between damping and spin torque is illustrated in equation (47).

This idea of divergence of spin torque as switching ability was applied in section 3.1 to the particular case of a bistable metallic nanopillar with an external in-plane magnetic field perpendicular to its easy axis. This allowed us, for example, to understand the appearance of stability regions in the parameter space for the Slonczewski efficiency factor $g(\theta; P)$ (see equation (17)) which were absent in the g-constant stability diagram as a consequence of the shifting of the angle for which the divergence vanishes $\vartheta_*(P)$ (see Figure 2.2 and Figure 2.3).

In general we expect the idea of divergence of spin torque as switching ability to facilitate

- Understanding of some "unusual" switching regimes.
- Understanding of stability behavior for "non-trivial" spin torque functional forms.
- Alternative device engineering to obtain maximum switching efficiency.

We have also addressed the question of stabilization of magnetization orientations corresponding to saddle points. This stabilization requires a change in the sign of the determinant of the stability matrix (see equation (37) and Table 2.1). Poincaré index theorem, nevertheless, constrains the stabilization process of a saddle point requiring another equilibrium to be involved in the process. As a consequence, in the generic case, saddles are not stabilized but simply merge with a center as the current is increased [1].

However, under special conditions saddles can be stabilized by increasing the current either in a process in which they exchange their stability nature with distant equilibria or in a collision-like process with an approaching stable equilibrium. This collision-like process is a transcritical bifurcation, and occurs whenever the direction of the polarizer coincides with that of a saddle point of magnetic energy. The critical bifurcation current can be analytically related to the determinant of the stability matrix associated with the magnetic torque as shown in equation (58).

[1] Both equilibria will disappear for currents larger than the critical merging current

Finally, we have illustrated the saddle point stabilization problem in the spin flip transistor, both when the saddles exchange their stability with distant equilibria (no external magnetic field, $\omega_H = 0$) and when they merge with approaching centers (finite external magnetic field, $\omega_H \neq 0$) as the current increases.

Bibliography

Arfken, G. B. (1995). *Mathematical Methods for Physicists* (Fourth ed.). San Diego, CA: Academic Press.

Ashcroft, N. and D. Mermin (1976). *Solid State Physics*. Thomson Learning.

Baibich, M. N., J. M. Broto, A. Fert, F. N. Van Dau, F. Petroff, P. Etienne, G. Creuzet, A. Friederich, and J. Chazelas (1988). Giant magnetoresistance of (001)fe/(001)cr magnetic superlattices. *Physical Review Letters 61*(21), 2472–2475.

Bauer, G., Y. Nazarov, and A. Brataas (2001). Spin-flip transistor. *Physica E-Low-Dimensional Systems & Nanostructures 11*(2-3), 137–143.

Bazaliy, Y., B. Jones, and S. Zhang (1998). Modification of the Landau-Lifshitz equation in the presence of a spin-polarized current in colossal- and giant-magnetoresistive materials. *Physical Review B 57*(6), R3213–R3216.

Bazaliy, Y., B. Jones, and S. Zhang (2004). Current-induced magnetization switching in small domains of different anisotropies. *Physical Review B 69*(9).

Bazaliy, Y. B. (2007). Magnetization dynamics in planar spin transfer devices and stabilization by repulsion in a spin-flip transistor. *Applied Physics Letters 91*(26).

Berger, L. (1996). Emission of spin waves by a magnetic multilayer traversed by a current. *Physical Review B 54*(13), 9353–9358.

Berkov, D. and J. Miltat (2008). Spin-torque driven magnetization dynamics: Micromagnetic modeling. *Journal of Magnetism and Magnetic Materials 320*(7), 1238 – 1259.

Binasch, G., P. Grünberg, F. Saurenbach, and W. Zinn (1989). Enhanced magnetoresistance in layered magnetic structures with antiferromagnetic interlayer exchange. *Physical Review B 39*(7), 4828–4830.

Bonin, R., C. Serpico, G. Bertotti, I. D. Mayergoyz, and M. d'Aquino (2007). Analytical study of magnetization dynamics driven by spin-polarized currents. *European Physical Journal B 59*(4), 435–445.

Brataas, A., G. Bauer, and P. Kelly (2006). Non-collinear magnetoelectronics. *Physics Reports-Review Section of Physics Letters 427*(4), 157–255.

Bruno, P. and C. Chappert (1991). Oscillatory coupling between ferromagnetic layers separated by a nonmagnetic metal spacer. *Physical Review Letters 67*(12), 1602–1605.

Crawford, J. (1991). Introduction to Bifurcation-Theory. *Reviews of Modern Physics 63*(4), 991–1037.

Garzon, S., L. Ye, R. A. Webb, T. M. Crawford, M. Covington, and S. Kaka (2008). Coherent control of nanomagnet dynamics via ultrafast spin torque pulses. *Physical Review B 78*(18), 180401.

Haney, P. M., R. A. Duine, A. S. Nunez, and A. H. MacDonald (2008). Current-induced torques in magnetic metals: Beyond spin-transfer. *Journal of Magnetism and Magnetic Materials 320*(7), 1300–1311.

Krivorotov, I. N., N. C. Emley, J. C. Sankey, S. I. Kiselev, D. C. Ralph, and R. A. Buhrman (2005). Time-Domain Measurements of Nanomagnet Dynamics Driven by Spin-Transfer Torques. *Science 307*(5707), 228–231.

Landau, L. D. and E. M. Lifshitz (1984). *L. D. Landau and E. M. Lifshitz Course on Theoretical Physics, Volume 8: Electrodynamics of Continuous Media* (Second ed.). Pergamon.

Lifshitz, E. M. and L. P. Pitaevskii (1981). *L. D. Landau and E. M. Lifshitz Course on Theoretical Physics, Volume 9: Statistical Physics, Part 2: Theory of the Condensate State*. Pergamon.

Mancoff, F., R. Dave, N. Rizzo, T. Eschrich, B. Engel, and S. Tehrani (2003). Angular dependence of spin-transfer switching in a magnetic nanostructure. *Applied Physics Letters 83*(8), 1596–1598.

Morise, H. and S. Nakamura (2005). Stable magnetization states under a spin-polarized current and a magnetic field. *Physical Review B 71*(1).

Myers, E., D. Ralph, J. Katine, R. Louie, and R. Buhrman (1999). Current-induced switching of domains in magnetic multilayer devices. *Science 285*(5429), 867–870.

Parkin, S. P. (2004). Shiftable magnetic shift register and method of using the same. *United States Patent* (6,834,005).

Parkin, S. S. P., M. Hayashi, and L. Thomas (2008). Magnetic domain-wall racetrack memory. *Science 320*(5873), 190–194.

Parkin, S. S. P., N. More, and K. P. Roche (1990). Oscillations in exchange coupling and magnetoresistance in metallic superlattice structures: Co/ru, co/cr, and fe/cr. *Physical Review Letters 64*(19), 2304–2307.

Ralph, D. C. and M. D. Stiles (2008). Spin transfer torques. *Journal of Magnetism and Magnetic Materials 320*(7), 1190–1216.

Slonczewski, J. C. (1996). Current-driven excitation of magnetic multilayers. *Journal of Magnetism and Magnetic Materials 159*(1-2), L1 – L7.

Smith, N., J. Katine, J. Childress, and M. Carey (2005). Angular dependence of spin torque critical currents for CPP-GMR read heads. *IEEE Transactions on Magnetics 41*(10), 2935–2940.

Sodemann, I. and Y. Bazaliy (2009). Anomalous stabilization in a spin-transfer system at high spin polarization. *Journal of Applied Physics 105*(7), 07D114.

Stiles, M. and A. Zangwill (2002). Anatomy of spin-transfer torque. *Physical Review B 66*(1).

Sukhov, A. and J. Berakdar (2009). Local Control of Ultrafast Dynamics of Magnetic Nanoparticles. *Physical Review Letters 102*(5).

Sun, J. (1999). Current-driven magnetic switching in manganite trilayer junctions. *Journal of Magnetism and Magnetic Materials 202*(1), 157–162.

Sun, J. (2000). Spin-current interaction with a monodomain magnetic body: A model study. *Physical Review B 62*(1), 570–578.

Sun, J. Z. and D. C. Ralph (2008). Magnetoresistance and spin-transfer torque in magnetic tunnel junctions. *Journal of Magnetism and Magnetic Materials 320*(7), 1227–1237.

Tserkovnyak, Y., A. Brataas, and G. E. W. Bauer (2002). Spin pumping and magnetization dynamics in metallic multilayers. *Physical Review B 66*(22), 224403.

Tsoi, M., A. Jansen, J. Bass, W. Chiang, M. Seck, V. Tsoi, and P. Wyder (1998). Excitation of a magnetic multilayer by an electric current. *Physical Review Letters 80*(19), 4281–4284.

Wang, X., G. Bauer, and T. Ono (2006). Current-controlled magnetization dynamics in the spin-flip transistor. *Japanese Journal af Applied Physics Part 1-Regular Papers Brief Communications & Review Papers 45*(5A), 3863–3868.

Wegrowe, J., D. Kelly, Y. Jaccard, P. Guittienne, and J. Ansermet (1999). Current-induced magnetization reversal in magnetic nanowires. *Europhysics Letters 45*(5),

626–632.

Xiao, J., A. Zangwill, and M. Stiles (2004). Boltzmann test of Slonczewski's theory of spin-transfer torque. *Physical Review B 70*(17).